AD-A059 641 NORTHWESTERN UNIV EVANSTON ILL DEPT OF CHEMISTRY F/G 7/2
RATIONAL SYNTHESIS OF UNIDIMENSIONAL MIXED VALENCE SOLIDS. STRU--ETC(U)
AUG 78 M A COWIE, A GLEIZES, G W GRYNKEWICH N00014-77-C-0231
UNCLASSIFIED TR-5 NL

1 OF 2
AD A059641

OFFICE OF NAVAL RESEARCH

Contract N00014-77-C-0231
Task No. NR 053-640

TECHNICAL REPORT NO. 5

Rational Synthesis of Unidimensional Mixed Valence Solids. Structural, Spectral, and Electrical Studies of Charge Distribution and Transport in Partially Oxidized Nickel and Palladium Bisdiphenylglyoximates.

by

Martin A. Cowie, Alain Gleizes, Gregory W. Grynkewich, Davida Webster Kalina, Malcolm S. McClure, Raymond P. Scaringe Robert C. Teitelbaum, Stanley L. Ruby, James A. Ibers Carl R. Kannewurf, and Tobin J. Marks

Prepared for Publication

in

The Journal of the American Chemical Society

Northwestern University
Department of Chemistry
Evanston, Illinois 60201

August 22, 1978

unclassified

SECURITY CLASSIFICATION OF THIS PAGE (When Data Entered)

REPORT DOCUMENTATION PAGE		READ INSTRUCTIONS BEFORE COMPLETING FORM
1. REPORT NUMBER Technical Report No. 5	2. GOVT ACCESSION NO.	3. RECIPIENT'S CATALOG NUMBER
4. TITLE (and Subtitle) Rational Synthesis of Unidimensional Mixed Valence Solids. Structural, Spectral, and Electrical Studies of Charge Distribution and Transport in Partially oxidized Nickel and+		5. TYPE OF REPORT & PERIOD COVERED Interim, 1978 6. PERFORMING ORG. REPORT NUMBER
7. AUTHOR(s) M.A. Cowie, A. Gleizes, G.W. Grynkewich, D.W. Kalina, M.S. McClure, R.P. Scaringe, R.C. Teitelbaum, S.L. Ruby, J.A. Ibers, C.R. Kannewurf, T.J. Marks		8. CONTRACT OR GRANT NUMBER(s) N00014-77-C-0231
9. PERFORMING ORGANIZATION NAME AND ADDRESS Department of Chemistry Northwestern University, Evanston, IL 60201		10. PROGRAM ELEMENT, PROJECT, TASK AREA & WORK UNIT NUMBERS NR-053-640
11. CONTROLLING OFFICE NAME AND ADDRESS Office of Naval Research Dept. of the Navy, Arlington, VA 22217		12. REPORT DATE August 22, 1978 13. NUMBER OF PAGES 88
14. MONITORING AGENCY NAME & ADDRESS(if different from Controlling Office)		15. SECURITY CLASS. (of this report) unclassified 15a. DECLASSIFICATION/DOWNGRADING SCHEDULE

16. DISTRIBUTION STATEMENT (of this Report)

Approved for public release; distribution unlimited

17. DISTRIBUTION STATEMENT (of the abstract entered in Block 20, if different from Report)

18. SUPPLEMENTARY NOTES

19. KEY WORDS (Continue on reverse side if necessary and identify by block number)

Polyiodide
Mixed valence material
Resonance Raman
Iodine Mössbauer
Diphenylglyoximate
Electrical conductivity
Polyiodide

20. ABSTRACT (Continue on reverse side if necessary and identify by block number)

This paper presents a detailed study of solid state structure, oxidation state, and electron transport in $Ni(dpg)_2I$ and $Pd(dpg)_2I$, dpg = diphenylglyoximato. The crystal structure of $Ni(dpg)_2I$ has been studied by x-ray diffraction at 23° and -160° C. The compound crystallizes from o-dichlorobenzene in the tetragonal space group D^8_{4h} - P4/ncc, with four formula units of $Ni(dpg)_2I$ in a unit cell having dimensions at -160° C of a = 19.774(8)Å c = 6.446(3)Å. Full-matrix least-squares refinement of 31 variables gave a

DD FORM 1 JAN 73 1473 EDITION OF 1 NOV 65 IS OBSOLETE S/N 0102-014-6601 |

unclassified

SECURITY CLASSIFICATION OF THIS PAGE (When Data Entered)

+Palladium Bisdiphenylglyoximates.

final value of the conventional R index (on F) of 0.093 for 353 reflections having $F_o^2 > 3\sigma(F_o^2)$. The crystal structure consists of stacked $Ni(dpg)_2$ units (staggered by 90°) and disordered chains of iodine atoms extending in the c direction. At 23° C the Ni-Ni separation is 3.271(1)Å (3.223(2)Å at -160°); other important distances are Ni-N = 1.868(15)Å; N-C = 1.33(3)Å; N-O = 1.34(3)Å. The $Ni(dpg)_2$ moiety is decidedly nonplanar (D_2 symmetry) with coordinated N atoms displaced 0.12(2)Å above or below the mean molecular plane. The form of iodine present, i.e., I_2, I^-, I_3^-, I_5^-, or mixtures thereof, cannot be determined from the Bragg scattering; analysis of diffuse x-ray scattering associated with the disordered iodine chains is consistent with I_5^- being the predominant species. This result is in agreement with resonance Raman spectroscopic studies on $Ni(dpg)_2I$ and $Pd(dpg)_2I$ as well as on an extensive series of selected model compounds. Fundamental polyiodide transitions in the $M(dpg)_2I$ materials are observed (ν_0 = 4880-6471Å) at 161 vs and 107w cm^{-1}; weak $M(dpg)_2$ - centered scattering is also noted. Iodine-129 Mössbauer data on $Ni(dpg)_2{}^{129}I$ and $Pd(dpg)_2{}^{129}I$ are also in best agreement with the I_5^- formulation. Averaging the data for both compounds, three sites with relative populations 2.04(10): 2.00(10): 1.00 are observed with isomer shifts (vs. ZnTe) = 1.20(3), 0.52(5), 0.18(1) mm/sec. and e^2qQ = -1764(5), -1331(8), -880(6) MHz, respectively. Thus, the $M(dpg)_2$ units are formally in fractional oxidation states of +0.20(4). Optical data show transitions at 566 nm ($Ni(dpg)_2I$) and 505 nm ($Pd(dpg)_2I$) which are most likely associated with the $M(dpg)_2$ stacking interaction, and a broad band in both materials at 675 nm which is assigned to the polyiodide chains. X-ray photoelectron spectra (Ni $2p_{3/2}$, Pd $3d_{3/2}$, $3d_{5/2}$) show no evidence of trapped valence. Single crystal electrical conductivity (both dc and 100 Hz ac) in the c (chain) direction is as high at 300° C as 1.1 x 10^{-1} $(\Omega\text{-cm})^{-1}$ ($Ni(dpg)_2I$) and 4.7 x 10^{-3} $(\Omega\text{-cm})^{-1}$ ($Pd(dpg)_2I$). Iodination brings about an increase in conductivity of > 10^8(Ni) and > 10^7(Pd), which is especially noteworthy since the only major change in crystal structure upon iodination is a ca. 0.27Å decrease in the $M(dpg)_2$ stacking distance. Variable temperature studies show the $Ni(dpg)_2I$ and $Pd(dpg)_2I$ conductivities to be thermally activated, with activation energies of 0.19 ± 0.01 eV and 0.54 ± 0.11 eV, respectively.

Contribution from the Department of Chemistry, the Department of Electrical Engineering, and the Materials Research Center
Northwestern University
Evanston, Illinois 60201
and the Physics Division
Argonne National Laboratory
Argonne, Illinois 60439

RATIONAL SYNTHESIS OF UNIDIMENSIONAL MIXED VALENCE SOLIDS. STRUCTURAL, SPECTRAL, AND ELECTRICAL STUDIES OF CHARGE DISTRIBUTION AND TRANSPORT IN PARTIALLY OXIDIZED NICKEL AND PALLADIUM BISDIPHENYLGLYOXIMATES.

by Martin A. Cowie,[1a] Alain Gleizes,[1a] Gregory W. Grynkewich,[1a] Davida Webster Kalina,[1a] Malcolm S. McClure,[1b] Raymond P. Scaringe,[1a] Robert C. Teitelbaum,[1a, 1d] Stanley L. Ruby,[1c] James A. Ibers*[1a] Carl R. Kannewurf,*[1b] and Tobin J. Marks*[1a, 2]

ABSTRACT

This paper presents a detailed study of solid state structure, oxidation state, and electron transport in $Ni(dpg)_2I$ and $Pd(dpg)_2I$, dpg = diphenylglyoximato. The crystal structure of $Ni(dpg)_2I$ has been studied by x-ray diffraction at 23° and -160° C. The compound crystallizes from o-dichlorobenzene in the tetragonal space group D_{4h}^8- P4/ncc, with four formula units of $Ni(dpg)_2I$ in a unit cell having dimensions at -160°C of a = 19.774(8)Å c = 6.446(3)Å. Full-matrix least-squares refinement of 31 variables gave a final value of the conventional R index (on F) of 0.093 for 353 reflections having $F_o^2 > 3\sigma(F_o^2)$. The crystal structure consists of stacked $Ni(dpg)_2$ units (staggered by 90°) and disordered chains of iodine atoms extending in the c direction.

At 23° C the Ni-Ni separation is 3.271(1)Å (3.223(2)Å at -160°); other important distances are Ni-N = 1.868(15) Å; N-C = 1.33(3)Å; N-O = 1.34(3)Å. The $Ni(dpg)_2$ moiety is decidedly nonplanar (D_2 symmetry) with coordinated N atoms displaced 0.12(2)Å above or below the mean molecular plane. The form of iodine present, i.e., I_2, I^-, I_3^-, I_5^-, or mixtures thereof, cannot be determined from the Bragg scattering; analysis of diffuse x-ray scattering associated with the disordered iodine chains is consistent with I_5^- being the predominant species. This result is in agreement with resonance Raman spectroscopic studies on $Ni(dpg)_2I$ and $Pd(dpg)_2I$ as well as on an extensive series of selected model compounds. Fundamental polyiodide transitions in the $M(dpg)_2I$ materials are observed (ν_0 = 4880-6471Å) at 161 vs and 107w cm^{-1}; weak $M(dpg)_2$ - centered scattering is also noted. Iodine-129 Mössbauer data on $Ni(dpg)_2{}^{129}I$ and $Pd(dpg)_2{}^{129}I$ are also in best agreement with the I_5^- formulation. Averaging the data for both compounds, three sites with relative populations 2.04(10): 2.00(10): 1.00 are observed with isomer shifts (vs. ZnTe) = 1.20(3), 0.52(5), 0.18(1) mm/sec. and e^2qQ = -1764(5), -1331(8), -880(6) MHz, respectively. Thus, the $M(dpg)_2$ units are formally in fractional oxidation states of +0.20(4). Optical data show transitions at 566 nm ($Ni(dpg)_2I$) and 505 nm ($Pd(dpg)_2I$)which are most likely associated with the $M(dpg)_2$ stacking interaction, and a broad band in both materials at 675 nm which is assigned to the polyiodide chains. X-ray photoelectron spectra (Ni $2p_{3/2}$, Pd $3d_{3/2}$, $3d_{5/2}$) show no evidence of

trapped valence. Single crystal electrical conductivity (both dc and 100 Hz ac) in the c (chain) direction is as high at 300°C as $1.1 \times 10^{-1} (\Omega\text{-cm})^{-1}$ ($Ni(dpg)_2I$) and 4.7×10^{-3} $(\Omega\text{-cm})^{-1}$ ($Pd(dpg)_2I$). Iodination brings about an increase in conductivity of $> 10^8$ (Ni) and $>10^7$ (Pd), which is especially noteworthy since the only major change in crystal structure upon iodination is a ca. 0.27Å decrease in the $M(dpg)_2$ stacking distance. Variable temperature studies show the $Ni(dpg)_2I$ and $Pd(dpg)_2I$ conductivities to be thermally activated, with activation energies of 0.19 ± 0.01 eV and 0.54 ± 0.11 eV, respectively.

Solids with strongly unidimensional structural and electronic interactions have attracted much recent attention among chemists and physicists[3]. New materials with quasi-metallic electrical, optical and magnetic properties concentrated largely in one (or two) dimension(s) have forced a progressive refinement of theoretical models as well as experimental expectations for cooperative phenomena in molecular solids. The ultimate goal of such research is to develop theory and chemical methodology to the point that such cooperative phenomena can be varied at will.

It has been our interest to explore general approaches to the chemical synthesis of quasi-metallic assemblages composed of molecular stacks or chains, and to employ the physical properties of the resulting designed materials to test current ideas regarding electron transport phenomena. Judging from what is presently known about highly conductive stacked systems such as KCP [$K_2Pt(CN)_4Br_{0.30} \cdot 3H_2O$], TTF - TCNQ, as well as others which do not undergo a low temperature transition to the semiconducting state[3,4], it is reasonable to attempt to array, in close proximity, flat, highly delocalized, polarizable molecules[3,5]. It is assumed, of course, that the stacked components occupy sites which are crystallographically as similar as possible. A crucial feature which also appears to be inextricably connected with facile electron transport, and which is understandable within the framework of the one-dimensional Hubbard

band model[3], is mixed valency[3,6]. That is, the molecular units to be connected in series must have fractional formal oxidation states. One plausible approach[7a] which we have investigated to ensure mixed valency has been to attempt to co-crystallize stacks of planar donor molecules, D, with an array of suitable acceptor species, A, which

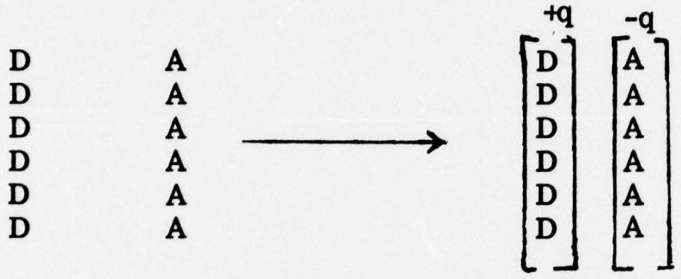

D = donor
A = acceptor

would each remove a non-integral amount of electronic charge per D unit ("partial oxidation"). The A moieties should be polarizable and must be sufficiently compact to pack easily within the assembly of D_n stacks. To promote mixed valency A must form stable polynuclear anions, A_n^{-1}.[7a] Thus, in the hypothetical material $DA_{1.0}$, each A would increase the formal oxidation state of each D by +1/n.

Our efforts to synthesize mixed valence structures by the above strategy have so far focussed primarily on the use of iodine as an acceptor[7,8]. Polyiodides such as I_3^{-1} and I_5^{-1} exhibit high thermodynamic stability in nonpolar media similar to environments expected in many D_n lattices and possess shapes which should not drastically restrict the formation of one-dimensional arrays[9]. Furthermore, iodine-containing oxidants are

readily amenable to characterization by the powerful combination of resonance Raman and iodine-129 Mössbauer spectroscopy[7, 10]. Thus, in a material of stoichiometry DI, identifying the iodine as I_2, I^{-1}, I_3^{-1}, I_5^{-1}, or a combination thereof allows a direct and accurate estimation of the electronic charge transferred from D to the acceptor. Such charge distribution information is of great importance in formulating models for electron transport and is not readily available for non-crystalline, microcrystalline, or severely disordered materials[3].

The earliest recognized examples of stacked, square planar metal complexes were the bisglyoximates of nickel, palladium, and platinum, A[11]. *It has been known for some*

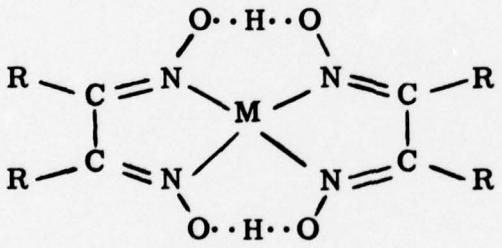

A

R = CH_3 : $M(dmg)_2$
R = C_6H_5: $M(dpg)_2$
M = Ni, Pd, Pt

time that the nickel and palladium bisdiphenylglyoximates can be reversibly iodinated (or brominated),as illustrated in equation (1)[12]. The products are lustrous

$$M(dpg)_2 + \tfrac{1}{2}I_2 \rightleftharpoons M(dpg)_2I \qquad (1)$$

M = Ni, Pd

golden-olive needles which exhibit weak temperature-independent paramagnetism and pressed pellet electrical conductivities which are ca. 10^4 greater than in the unhalogenated materials[13]. Subsequent studies have inferred the basic one-dimensional nature of the $M(dpg)_2I$ crystal structure and have thoroughly categorized the range of stoichiometries and halogenation products which exist[14]. However, this information did not resolve the fundamental question of whether these materials were or were not mixed valent, and the form of the iodine was variously formulated as I_2 (formally Ni^{+2}, a halogen charge-transfer complex[15]), I^{-1} (formally Ni^{+3}[16]), and I_3^{-1} (formally $Ni^{+2.33}$, partially oxidized[14c]). It was of great interest to us to investigate the $M(dpg)_2I$ systems in greater detail as the first prototypes of mixed valence lattices synthesized via the polyiodide strategy. In this paper we present a full exposition of our structural, spectral, and electron transport measurements on the nickel and palladium bisdiphenylglyoximato iodides. It is unequivocally demonstrated that these systems do contain $M(dpg)_2$ units in formal fractional oxidation states, and that the spectral methods for charge distribution analysis have wide applicability. In so doing we revise, on the basis of improved spectroscopic and diffraction data, our original suggestion[7c,d] that the iodine-containing species is largely I_3^- in these systems; rather we show that it is largely if not exclusively I_5^-. In a companion paper[7b] we examine the structural and electronic characteristics of the more closely coupled and highly conjugated nickel and palladium bisbenzoquinonedioximato iodides, which provide further insight into the response of stacked metal dioximate systems to partial oxidation.

EXPERIMENTAL

Elemental analyses were performed by Ms. H. Beck, Northwestern Analytical Services Laboratory, or Micro-Tech Laboratories. All halogenated samples were stored in closed vials in a freezer at -20° C.

Synthesis of $M(dpg)_2I$ Compounds, M = Ni, Pd. Bis(diphenylglyoximato) Ni(II) was prepared by reaction of diphenylglyoxime (Eastman) with $NiCl_2 \cdot 6H_2O$ in refluxing ammoniacal ethanol[14a]. Bis(diphenylglyoximato) Pd(II) was prepared in a similar manner using $PdCl_2$[14b]. Both complexes were purified by several recrystallizations from hot dimethylformamide. The corresponding iodides were prepared by reacting o-dichlorobenzene solutions of the metal diphenylglyoximates (ca. 10^{-3}M) at 110° C with a ca. 35-150 fold molar excess of triply sublimed I_2. The hot solution was gravity filtered, rewarmed to 110° C, and then slowly cooled to room temperature in an insulated dewar flask over a period of 3-5 days. The golden-olive crystals obtained were collected by suction filtration and were washed with pentane until the washings were colorless. Yields by this procedure ranged from 40-60%.

Anal. Calcd. for $Ni(C_{14}H_{11}O_2N_2)_2I$: C, 50.63; H, 3.34; N, 8.44; I, 19.11. Found: C, 50.92; H, 3.10; N, 8.39; I, 19.37. Calcd. for $Pd(C_{14}H_{11}O_2N_2)_2I$: C, 47.24; H, 3.12; N, 7.87; I, 17.83. Found: C, 47.04; H, 3.13; N, 7.75; I, 17.30.

Complete infrared spectra (Nujol mulls, cm^{-1}):

$Ni(dpg)_2$: 3090vw. 3075w, 3060mw, 1985vw, 1965vw, 1895vw, 1805vw, 1765vw, 1600vw, 1580mw, 1530vs, 1490vs, 1445vs, 1320w, 1290s, 1210m, 1155mw, 1140vw, 1070m, 1000mw, 970n; 930ms, 900s, 850m, 810n, 775ms, 740vs, 690vs, 670w, 384w, 323vs, 295s, 248w, 176vs, 130-140m,

$Ni(dpg)_2I$: 3075w, 1965vw, 1820vs, 1600mw, 1580w, 1530m, 1490s, 1445vs, 1330m, 1295s, 1280ms, 1220w, 1155mw, 1140vs, 1070mw, 1025w, 975mw, 930ms, 900s, 850mw, 820w, 770s, 740s, 690vs, 670mw, 388m, 365vs, 319s, 298vs, 260w, 174vs, 130-140s.

$Pd(dpg)_2$: 3090vw, 3070w, 3060mw, 1985vw, 1965vw, 1895vs, 1810vw, 1765vw, 1600vs, 1580mw, 1520m, 1490s, 1445vs, 134mw, 1325m, 1300s, 1280m, 1190mw, 1160ms, 1140mw, 1070m, 1025ms, 1000m, 970ms, 930m, 885s, 840mw, 815mw, 760mw, 740vs, 690vs.

$Pd(dpg)_2I$: 3070w, 1975vw, 1900vw, 1820vw, 1590mw, 1570mw, 1510mw, 1485m, 1440vs, 1345m, 1335m, 1305s, 1280m, 1155m, 1135m, 1070mw, 1025m, 1000w, 970mw, 920mw, 880s, 845w, 810w, 765s, 740vs, 690vs.

The above synthetic procedure was found consistently to produce the largest $M(dpg)_2I$ crystals; however, overall yields were diminished somewhat. Larger yields of the $M(dpg)_2I$ materials can be obtained by using more concentrated solutions, but more rapid crystallization and smaller crystals result. With a deficiency of iodine, dilute or concentrated solutions yield products which, by optical microscopy, are seen to be mixtures of light and dark-colored crystals. Mechanical separation and elemental analysis show these to be the $M(dpg)_2$ and $M(dpg)_2I_{1.0}$ derivatives, respectively.

Synthesis of $M(dpg)_2{}^{129}I$ Compounds, M = Ni, Pd. For the $Ni(dpg)_2{}^{129}I$ and $Pd(dpg)_2{}^{129}I$ Mössbauer samples, the above procedure was carried out on a smaller scale using more concentrated o-dichlorobenzene solutions and a ca. 7 molar excess of $^{129}I_2$. The latter reagent was prepared by oxidizing acidified $Na^{129}I$ solutions (Oak Ridge National Laboratory) with 30% H_2O_2 and extracting the iodine into o-dichlorobenzene. The organic layer was next separated, washed twice with distilled water, and dried over anhydrous Na_2SO_4. This solution was then used for $M(dpg)_2$ iodination.

Synthesis of $M(dpg)_2Br$ Compounds, M = Ni, Pd. The compounds $Ni(dpg)_2Br$ and $Pd(dpg)_2Br$ were prepared by reacting the $M(dpg)_2$ compounds in CCl_4 with Br_2 as described by Edelman[12]. These compounds lose halogen at room temperature far more rapidly than do the iodides.

Complete infrared spectra (Nujol mulls, cm^{-1}):

$Ni(dpg)_2Br$: 3075w, 1970vw, 1820vw, 1600mw, 1575w, 1525mw, 1490s, 1445vs, 1330m, 1295s, 1280ms, 1155m, 1140vs, 1100mw, 1070mw, 1025w, 1000w, 975mw, 930m, 900ms, 850w, 770s, 740s, 690vs, 670mw, 388m, 363s, 320ms, 298s, 261w, 173vs, 110-140s.

$Pd(dpg)_2Br$: 3075w, 1970vw, 1820vw, 1595mw, 1575w, 1515w, 1485m, 1440vs, 1335m, 1300s, 1275m, 1150m, 1140m, 1070w, 1025m, 1000w, 975w, 925mw, 880s, 840vw, 805vw, 775w, 765s, 740vs, 690vs.

Raman Measurements Laser Raman spectra were recorded with Kr^+(6471Å) or Ar^+(4880Å, 5145Å) excitation using a Spex 1401 monochromator and photon counting

detection. The solid samples were studied in 5 or 12 mm Pyrex sample tubes spinning at 1200 rpm. A 180° back-scattering geometry was employed. A number of scans were made of each sample (the initial at lowest laser power) to check for possible sample decomposition. Spectra were calibrated with the exciting line (ν_0) or laser plasma lines. For variable temperature studies the spinning sample was placed in a transparent glass dewar and was cooled in a stream of boil-off nitrogen. Temperatures were calibrated with a copper-constantan thermocouple. Spectra at ca. 8° K were obtained using an apparatus described elsewhere.[17]

Infrared Measurements Routine infrared spectra were recorded with a Perkin-Elmer model 267 spectrophotometer. Far-infrared spectra were obtained with a Perkin-Elmer model 180 instrument. Samples were studied as Nujol mulls between KBr or polyethylene plates. The far-infrared studies were performed with a thorough and continuous purge of dry nitrogen.

Iodine-129 Mössbauer Spectroscopy For Mössbauer measurements, source, absorber and detector were employed in the standard transmission geometry. The $^{66}Zn^{129}Te$ source ($t_{\frac{1}{2}}$ = 70 min.) was prepared by irradiation of a $^{66}Zn^{128}Te$ target (pressed in an aluminum disk) in the Argonne CP-5 reactor for 2 hr. The source produced sufficient 27.7 KeV γ-radiation for 3-4 hr. of Mössbauer effect data collection. Absorbers were prepared by powdering the iodine-129

enriched samples, mixing with an inert filler (boron nitride) and loading into Lucite sample holders. The absorbers typically contained ca. 30 mg. $^{129}I/cm^2$, which represents a compromise between large Mössbauer effect γ-ray absorption, self-absorption, Compton scattering, and thickness errors. Both the source and absorber were cooled to 4.2°K during data collection. Typically, 3-4 sources were used, in sequence, to collect all the data for a given sample. Data collected from each source were summed to give the final spectra. Individual runs were checked for reproducibility. Attempts to observe spectra with the sample at 77°K were unsuccessful, owing to the low ^{129}I recoilless fraction. The spectrometer velocity was generated with a feedback-controlled vibrator using sinusoidal acceleration. The velocity drive was calibrated with ^{57}Fe foil. Data were collected with a proportional counter in conjunction with a 400 channel multichannel analyzer operating in the time mode. Data were stored on paper tape.

Mössbauer effect data processing and analysis employed the computer program, GENFIT, which finds the best values of the parameters of isomer shift, quadrupole coupling constant, line width, populations, baseline and asymmetry parameter via least-squares minimization of the difference between the observed and calculated spectra. The goodness of fit is judged by the parameter "Misfit," which has been previously defined by Ruby.[18] "Misfit," which is a modification of the parameter χ^2,[19] is better suited to deciding which of several models fits several measurements more accurately.

The end sites in the pentaiodide ion showed large linewidths in comparison with the other iodine sites. This could be explained if the end sites have a distribution of quadrupole coupling constants. That is, not all end sites are exactly equivalent. This nonequivalence was incorporated in the fitting procedure as a velocity-dependent line-broadening function(eq(2)).

$$\Gamma_n = \sqrt{[\kappa (V_n - \delta)]^2 + \Gamma_{true}} \qquad (2)$$

where Γ_{true} is the actual line width, δ is the isomer shift, V_n is the velocity of line n, κ is the broadening parameter, and Γ_n is the observed velocity of the n^{th} line. This function broadens the lines furthest away from the center of gravity (δ, isomer shift) to a greater extent than those lines closer to δ. This has the same overall effect as a quadrupole distribution. Using this value of Γ_n, reasonable linewidths for all sites are obtained.

Electronic Spectra Spectra of solid samples were studied as Nujol mulls between quartz plates in a Cary 17-D spectrophotometer. Several scans were made of each sample to check for possible decomposition.

Single Crystal Conductivity Measurements Samples selected for electrical conductivity measurements had no apparent growth defects that could be observed by microscopic inspection. Typical sample dimensions for the tetragonal needles were 2.0 to 3.0 mm in length and 0.1 to 0.2 mm in thickness. All measurements were performed with current flow along the c-axis direction.

Mounting and electrode attachment employed the conventional four-probe technique. The substrate mounts were prepared from a typical integrated circuit header assembly before encapsulation. Small diameter gold or aluminum wires served as electrode connectors and were attached to the samples using either colloidal graphite suspended in 1,3-butylene glycol, or Demetron M8001 cold-setting conductive gold contact paint. Conductivity results with these two contact materials were identical. In addition, it was found that conductivities remained constant over a period of days at room temperature, indicating that no reaction was taking place between sample and contact material. Sample electrode arrangements were checked by the procedure of Schafer et. al.[20]

Current for dc conductivity measurements was supplied by a Keithley model 225 regulated current source; voltage was measured by two Keithley model 610 B electrometers in differential configuration. Several low frequency ac(100 Hz.) measurements were performed using PAR 124 and HR8 lock-in amplifiers. The results were in good agreement with the dc measurements. Variable temperature studies were conducted in a Delta Design environmental chamber. Temperatures were monitored with a copper- constantan thermocouple adjacent to the sample. Room temperature measurements were always made after high temperature ($\geq$ 300° K) studies to check for possible sample decomposition.

X-Ray Photoelectron Spectroscopy XPS spectra were recorded on an AEI-ES100B spectrometer using Al K_α radiation. Time averaging was performed with a PDP-85 data system. A least-squares fit of the data points

was achieved using the program SMOOTH II.[21] Spectra were recorded at room temperature. In order to check for possible loss of iodine from the $M(dpg)_2I$ compounds in the high vacuum of the spectrometer, the I 3d 5/2 peak was recorded at the beginning and end of each run; no drop in the intensity of this peak was observed. Furthermore, spectra recorded at -50° C were identical to those obtained at room temperature. Attempts at argon ion etching did, however, result in loss of iodine from the $M(dpg)_2I$ complexes and apparent reduction to $M(dpg)_2$ (even at low temperature). Binding energies reported are relative to C1s (taken to be 285.0 eV). The uncertainty in these numbers is somewhat large owing to the rather large shift (0.3 - 0.9 eV) in C1s kinetic energy observed in the course of the runs (a period of several hours), most likely a consequence of charging effects. An attempt was made to obtain the relative binding energies of $M(dpg)_2I$ vs. $M(dpg)_2$ by running a homogeneously mixed sample of the two materials. In each case, no splitting or broadening of the peaks was observed.

X-Ray Diffraction Study of $Ni(dpg)_2I$. Crystals of $Ni(dpg)_2I$, suitable for x-ray diffraction studies, were grown by the slow cooling of o-dichlorobenzene solutions containing an excess of iodine as described above. The crystals obtained are black, very thin needles with a silver, metallic lustre. The crystal structure of $Ni(dpg)_2I$, based on diffractometer data collected at room temperature, has been described.[7c,d] In an attempt to characterize more fully the nature of the iodine-containing species, a low-temperature study has been carried out.

For the low temperature study a suitable, although rather small crystal was mounted with G. E. Glyptal to a copper fiber (diameter = 0.5mm) in an Air Products Cryo-tip goniometer equipped with a closed Joule-Thomson cooling cycle. The crystals have the same space group at both 23° C and -160° C. Accurate cell parameters at -160(5)° C were obtained by a least-squares analysis of the setting angles of 13 hand-centered reflections chosen from diverse regions of reciprocal space ($29.0° \leq 2\theta \leq 57.1°$, $CuK\alpha_1$ radiation) and obtained using a narrow x-ray source. Table I contains pertinent crystal data for the low temperature study.

The low temperature data were collected on a Picker four-circle automated diffractometer as has previously been described.[22] The intensities of six standard reflections were measured every 100 reflections to assess crystal movement or decomposition. There was no significant variation in these standards. The intensities of 1102 accessible reflections with indices $\ell \geq 0$ and $h \geq k \geq 0$ were measured for $2° \leq 2\theta \leq 120°$ using nickel-filtered Cu $K\alpha$ radiation. Of these, 416 have $F_o^2 \geq 3\sigma(F_o^2)$. The data were processed in the usual way using a value of 0.04 for p.[23] An absorption correction was applied to the data using Gaussian integration.[24]

Structure Solution and Refinement. The positions of all non-hydrogen atoms were taken from the room temperature determination,[7c] with the nickel

atoms on the 4(a) special positions and the iodine atoms on the 4(c) special positions in sqace group P4/ncc (with unit cell origin at $\bar{1}$). The structure was refined using full-matrix, least-squares techniques, minimizing the function $\Sigma w (|F_o| - |F_c|)^2$, where $|F_o|$ and $|F_c|$ are the observed and calculated structure amplitudes and the weights, w, are taken as $4F_o^2/\sigma^2(F_o^2)$. The agreement indices are defined as $R = \Sigma||F_o| - |F_c||/\Sigma|F_o|$ and $R_w = [\Sigma w(|F_o| - |F_c|)^2 / \Sigma wF_o^2]^{\frac{1}{2}}$. Atomic scattering factors were taken from the usual sources.[25] Anomalous dispersion terms[26] for the Ni and I atoms were included in F_c. A series of θ-2θ scans performed for $2^\circ \leq 2\theta \leq 110^\circ$ in several arbitrary crystal orientations indicated the regions of interference from the Cu powder pattern of the Cu fiber. These regions agree well with those calculated for copper scattering at -160° C. Owing to the low intensities of many reflections, these powder lines constitute a significant contribution to the observed intensities so all data in these regions of 2θ were eliminated from further refinements, leaving 353 reflections with $F_o^2 \geq 3\sigma(F_o^2)$. Although a difference Fourier synthesis enabled us to locate all the hydrogen atoms, their positions were idealized. A C-H distance of 0.95Å was assumed for the hydrogen atoms of the phenyl groups. The hydrogen atom of the hydroxyl group was placed on the crystallographic two-fold axis between the two oxygen atoms. Each hydrogen atom was assigned a thermal parameter of 1Å^2 greater than that of the atom to which it is attached.

In the low temperature structure all thermal parameters are, as expected, significantly lower than those at room temperature. However, as was found earlier,[7c]

the mean-square amplitude of vibration of the I atom in the c-direction (U_{33}) is approximately 10 times greater than it is normal to this direction.

For reasons to be discussed later, it is certain that the apparent high thermal motion of the iodine atoms is caused by a disorder in the iodine chain. Hence, there is a distribution of possible iodine atom positions in the cell. Under these circumstances the use of thermal parameters will not reproduce the observed electron density distribution unless one of the following is true:[27]

1) The magnitude of the displacements characteristic of the disorder is small.
2) The distribution of displacements (whether or not their magnitudes are small) is Gaussian.

Since in the present case neither of these conditions applies, several peaks in the difference Fourier map persisted throughout anisotropic refinement. The optimal solution to this problem would involve proposing a detailed model for the disorder and then reproducing the predicted electron density distribution by placing atoms with fractional occupancy factors in appropriate positions. However, to arrive at such a model based on the structureless mass of electron density along the line $\frac{1}{4}, \frac{1}{4}, z$ is obviously out of the question. In theory, a detailed disorder model can be deduced by interpretation of the diffuse scattering; efforts are being made in this direction and will be discussed later. An alternative approach is to approximate the observed electron density distribution by some function other than the Gaussian. We have applied this idea successfully to a similar structure,[28] but in the present case we have been unable to find a

distribution which yields results superior to those for the Gaussian.

In the final least-squares refinement only one I atom position was refined and the solution converged to values of R and R_w of 0.093 and 0.126, based on 31 variables and 353 observations. The error in an observation of unit weight is 4.03 electrons. An analysis of $\Sigma w(|F_o| - |F_c|)^2$ as a function of F_o, setting angles, and Miller indices shows no unusual trends apart from the poor agreement at low θ values. This is to be expected on the basis of the I atom disorder. The highest 15 peaks in a final difference Fourier synthesis are between the I atoms in the I chains (3.5-3.6(1)eÅ^{-3}), between the Ni atoms (1.3-1.5(2)eÅ^{-3}), near the oxygen atoms (0.9-1.0(2)eÅ^{-3}), and near the phenyl rings (0.7(2)eÅ^{-3}). The residuals between the I and Ni atoms are probably a consequence of the disorder of the I atoms, and the resulting poor refinement of the ordered model, although electron density errors are expected to be higher in special positions.

The final positional and thermal parameters appear in Tables II and III. Root-mean-square amplitudes of vibration of the I and Ni atoms at both 23° and -160° are given in Table IV. A listing of the observed and calculated structure amplitudes is available.[29]

Diffuse X-Ray Scattering Examination of ordinary oscillation photographs taken with nickel filtered Cu radiation revealed the presence of three weak layers at ca. 2.12, 2.44, and 2.80 reciprocal lattice units in addition to the normal Bragg layer lines. Subsequent stationary crystal photographs demonstrated that the extra scattering is concentrated in planes normal to the c axis. These observations clearly indicate the existence of one-dimensional disorder in this material. We identify the disorder with the iodine chain because of the apparent high thermal motion of the iodine atoms and because the resulting model (I^-

ion separated by ~3.26 Å) is physically unrealistic. The intensity in any given diffuse layer is slightly modulated indicating that some three dimensional correlations are present between chains. Diffuse scattering similar to that observed here is well documented for materials containing iodine chains.[7a,8c,30] In these cases, the diffuse layers can be indexed on the basis of a 9.7Å superlattice and the interpretation of intensity data, when measured, yield disorder models involving the triiodide ion as the iodine containing species. In the present case this interpretation is not possible. In $Ni(dpg)_2I$, the observed layers (six are visible if photographs are taken with Mo radiation) can be roughly indexed on the basis of an 18.32Å repeat superlattice spacing, which corresponds to ca. (14/5) $\underline{c}$. We reject this interpretation because the agreement with calculated layer positions is rather poor, and because it is not possible to arrive at the observed electron density distribution on the basis of any model involving an incommensurate superlattice spacing of this length. Closer examination of the oscillation photographs shows that there is considerable broadening of the diffuse lines relative to the Bragg lines. This has been confirmed by counter measurements of the diffuse scattering pattern employing monochromatic CoK_α(λ = 1.7889Å) radiation. Irregular layer spacings and broadening is suggestive of a system displaying short-range order. An experimental example of this phenomenon has been reported for the one-dimensional material Hollandite.[31] We are currently analyzing the diffuse scattering pattern of Ni(dpg)I in terms of short-range order models.

Although optimization of the model is not yet complete, the agreement with experiment at present is sufficiently close that qualitative information about the iodine species in this material is now available.[28] In particular, all attempts to reproduce the observed scattering in terms of models with I_3^- or I_2 have been unsuccessful. The primary reason for this is that it is difficult, if not impossible, to postulate a sensible physical model based on these species which reproduces the main feature of the observed scattering pattern (the intense peak at 2.06 reciprocal lattice units). This is in agreement with the ^{129}I Mössbauer and resonance Raman results (see Results Section) which indicate that these species are either completely absent, or present in small amounts only. Of the numerous models considered thus far, only those involving I_5^-[32] as the predominate species have met with success in explaining the experimental data.

RESULTS AND DISCUSSION

Chemistry

The compounds $Ni(dpg)_2I$ and $Pd(dpg)_2I$ were prepared as shown in equation (1). Very slow cooling of hot o-dichlorobenzene solutions of the $M(dpg)_2$ complexes with a large excess of iodine produced lustrous golden-olive crystals of sufficient size for x-ray diffraction and electrical conductivity studies. Under the synthetic conditions employed, the metal:I ratio in the product was consistently found to be $1.00:1.00 \pm 0.05$. When deficiencies of iodine were employed, the slow cooling technique produced mixtures of $M(dpg)_2$ and $M(dpg)_2I$ crystals, which could be mechanically separated and characterized (see Experimental Section). There was also no evidence from laser Raman spectroscopy (vide infra) that

$M(dpg)_2I_x$ materials were present with x not 1.0 or 0.0. Likewise, the $M(dpg)_2I$ compounds were found to lose I_2 upon heating, and at no time during this process were Raman signals observed for materials other than x = 1.0 or x = 0.0.

Crystal Structure of $Ni(dpg)_2I$.

The structure of $Ni(dpg)_2I$ consists of discrete $Ni(dpg)_2$ units and I atoms with no unusual non-bonded contacts (see Table V). The $Ni(dpg)_2$ units are stacked along the crystallographic c axis with the coordination plane of the Ni atom perpendicular to the stacking direction. Each $Ni(dpg)_2$ unit is staggered by 90° with respect to its nearest neighbor along the stacking axis. The iodine atoms also stack one above the other in the c-direction, filling the "tunnels" created by the phenyl rings of the diphenylglyoximato ligands. The packing is shown in the stereoscopic view of the unit cell contents in Figure 1. Figure 2 shows stacking of the Ni and I atoms in the c direction. A drawing of the $Ni(dpg)_2$ unit showing relevant bond lengths and angles is presented in Figure 3.

The Ni atoms occupy the 4(a) special positions in the space group P4/ncc. Therefore, all Ni atoms are equally spaced along the stacking direction by c/2 (3.223(2) Å). This distance can be compared with the corresponding Ni-Ni distances in the stacked compounds $Ni(dpg)_2$(3.547Å),[14d] $Ni(dmg)_2$ (3.25Å),[11] $Ni(bqd)_2I_{0.02}$ (3.180(2)Å)[7b] where bqd = benzoquinonedioximate, $Ni(bqd)_2I_{0.5}$ (3.153(3)Å),[33] NiPc(4.79Å)[34] where Pc = phthalocyanine, and $NiPcI_{1.0}$ (3.244(3)Å).[7a, 8c] In all cases where an iodinated and non-iodinated material can be compared, the iodination has brought about a significant contraction in the Ni-Ni distance. Despite this contraction, the metal-metal

distances in these stacked compounds are still appreciably larger than in face-to-face metallomacrocycle dimers such as $[Ni(C_{14}H_{18}N_4)]_2(CF_3SO_3)_2$,[35] which contains two eclipsed B units. Here spectral studies[35a] suggest a weak metal-metal interaction, and the Ni-Ni distance is found to be 3.063(1)Å.[35b] Analogous examples include

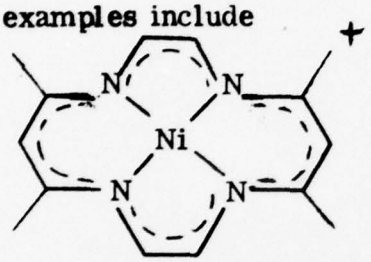

B

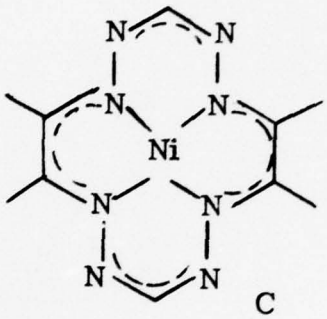

C

$[Ni(C_{10}N_{14}N_8)]_2$,[36] containing structural unit C, where there is considerably stronger metal-metal communication and where Ni-Ni = 2.788(2)Å, and $[Ni(dmgBF_2)_2]_2$[37] where Ni-Ni = 3.21Å. As a point of reference, the distance in nickel metal, 2.49Å,[38] is shorter still.

The $Ni(dpg)_2$ unit has crystallographically imposed point symmetry 222 so it is not crystallographically required to be planar. In fact, the molecule is rather puckered. This is shown clearly in Table VI by the deviations of the atoms from the least-squares planes. In plane 5, consisting of the four N atoms, each N atom is displaced alternately above and below the plane by 0.12(2)Å. Similarly, within the chelate ring the two C atoms are displaced above and below the mean plane by 0.20(3)Å. The large N-C-C'-N' torsion angle of 33(2)° about C-C' bond is a further indication of the non-planarity of the chelate ring. This puckering of the inner core of the $Ni(dpg)_2$ unit appears to

result from the close approach of the two adjacent phenyl groups on the chelate and also from the close approach of the molecules along the stacking axis. Table V shows that there are several short non-bonded contacts primarily involving the phenyl rings. The distortions of the C-C(1)-C(2) and C-C(1)-C(6) angles (see Table V) from their ideal values of 120° also seem to result from the above interactions. To minimize these interactions the adjacent phenyl rings are tipped 64.8° from each other and 36.8° from the chelate plane.

All bond lengths and angles in the $Ni(dpg)_2$ unit, at -160°C, are essentially identical to those in the room temperature structure determination[7c] and agree well with those reported in other nickel tetraazamacrocycle complexes. The $Ni(dpg)_2I$ results are of limited accuracy owing to the predominance of iodine scattering and the presence of diffuse intensities. The Ni-N distance of 1.868(15)Å is normal, being close to the value of ca. 1.85Å observed in several four-coordinate Ni(II) complexes.[39] This contact is significantly shorter than the Ni-N distances observed in the four-coordinate Ni(II) porphyrins (1.902(5) to 1.98(1)Å),[40-43] However, it is close to the average Ni-N distance of 1.874(3)Å in $[Ni(C_{14}H_{18}N_4)]_2(CF_3SO_3)_2$,[35b] and 2.788(2)Å in $[Ni(C_{10}H_{14}N_8)]_2$.[36] The N-C distance of 1.33(3)Å and the N-O distance of 1.34(3)Å in the coordinated diphenylglyoximate ligand are comparable to the corresponding distances in $Ni(dmg)_2$,[11] i.e., 1.30(3) and 1.35(2)Å, respectively. The distances C-C' (1.61(4)Å) and O-O(2.40(4)Å) in the present structure also compare favorably with the analogous $Ni(dmg)_2$ parameters of 1.54(3) and 2.40(2)Å, respectively.

As already noted in the discussion of the structure solution (Experimental Section) the iodine atoms in $Ni(dpg)_2I$ are disordered along the $\underline{c}$ axis in

such a manner that the form of the iodine (I_2, I_3^-, I_5^-, I^- or a mixture thereof) cannot be determined from the Bragg scattering. Analysis of the diffuse scattering pattern which is observed can, in principle, provide the desired structural information.[30, 44] Diffuse scattering data have been collected by counter methods for $Ni(dpg)_2I$. Analysis of these data is in progress. At the present time it is possible to reject models consisting of simple chains of I_2 or I_3^- units; the data are consistent with I_5^- being the predominant species. Spectral data (vide infra) are also consistent with the presence of I_5^- units.

Resonance Raman Studies

In an effort to obtain additional information on the nature of the iodine-containing species in $Ni(dpg)_2I$ and $Pd(dpg)_2I$, solid state resonance Raman[45] vibrational spectroscopic studies were undertaken. As will be seen, this method can provide valuable structural information on polyiodide molecular structure and is immune to diffraction-related problems such as disorder and non-crystallinity. Each type of polyiodide molecule gives rise to a characteristic Raman scattering spectrum, and the resonant enhancement with typical visible laser excitation frequencies is generally sufficient so that iodine-centered vibrational transitions are not obscured by modes from other oscillators in the crystal. A complete

description of our resonance Raman studies on a wide variety of polyiodide compounds will be presented elsewhere.[10c] In this discussion we summarize the theory and results pertinent to differentiating various species which could occur in the channels of low-dimensional materials such as $Ni(dpg)_2I$ and $Pd(dpg)_2I$.

The intensity of a Raman transition, $I(\nu_r)$, averaged over all molecular orientations, can be expressed in terms of the Raman scattering tensor, $R_{\rho\sigma}$, as shown in equation (3). Here $I(\nu_0)$

$$I(\nu_r) = \frac{2^7\pi^5}{3^2c^4}\ \nu_r^4 I(\nu_0) \sum_{\rho\sigma} \left|R_{\rho\sigma}\right|^2 \tag{3}$$

is the intensity of the laser exciting line (at ν_0), ν_r is the frequency of the Raman scattered radiation, and c is the speed of light. It is possible to express $R_{\rho\sigma}$ in such a way as to incorporate both Herzberg-Teller coupling and Born-Oppenheimer nonadiabatic coupling.[45,46] Thus, according to equation (4)

$$R_{\rho\sigma} = A + B \tag{4}$$

the Raman scattering tensor is the sum of terms which describe scattering arising from Franck-Condon allowed transitions involving a single excited electronic state (A terms) and those which derive intensity through vibronic coupling between two or more excited electronic states (B terms). For a transition from vibrational level i to j in the ground electronic state

(gi to gj), these terms can be expressed as in equations (5) and (6). Here

$$A = \frac{1}{h} \Sigma \left[\frac{(g^0|\mu_\rho|e^0)(e^0|\mu_\sigma|g^0)\langle gj|ev\rangle\langle ev|gi\rangle}{\nu_{ev,gi} - \nu_0 + i\Gamma_{ev}} + \frac{[\rho \leftrightarrow \sigma]}{\nu_{ev,gi} + \nu_0 + i\Gamma_{ev}} \right] \tag{5}$$

$$B = \frac{-1}{h^2} \sum_{e,v} \sum_{s,u}' \left[\frac{(g^0|\mu_\rho|s^0)(s^0|\partial H/\partial Q)_0|e^0)(e^0|\mu_\sigma|g^0)\langle gj|su\rangle\langle su|Q|ev\rangle\langle ev|gi\rangle}{(\nu_{su,gi} - \nu_0 + i\Gamma_{su})(\nu_{ev,gi} - \nu_0 + i\Gamma_{ev})} \right. \tag{6}$$

$$\left. + \frac{[\rho \leftrightarrow \sigma]}{(\nu_{su,gj} + \nu_0 + i\Gamma_{su})(\nu_{ev,gj} + \nu_0 + i\Gamma_{ev})} \right]$$

$|e^\circ)$ is the adiabatic electronic wave function of excited electronic state e, evaluated at the equilibrium nuclear coordinates of the ground electronic state, g, μ is the dipole transition operator, and $|ev\rangle$ is the wave function of vibrational level v of state e. The terms $\nu_{ev,gi}$ in the denominator are the frequency separation between vibronic levels and the Γ_{ev} denote damping terms describing the radiative widths of the vibronic states, ev. The symbol s denotes excited electronic states other than e, the prime on the summation excludes terms where s = e, and $(\partial H/\partial Q)_0$ represents the vibronic coupling operator describing how the electronic Hamiltonian varies with displacement along normal mode Q. This operator is evaluated at the ground state nuclear coordinates and transforms as normal mode Q. The second term in each equation refers to the non-resonant case. It is seen from equations (5) and (6) that for A terms, only the totally symmetric normal modes of molecular vibration are expected to be resonance enhanced, while for B terms only those vibrational modes which vibronically

couple states s and e are expected to be enhanced. Those normal modes which transform the molecule from the ground state nuclear configuration to an appreciably displaced nuclear configuration in an excited electronic state should, all other factors being equal, experience the greatest resonance enhancement.

In addition to the above relationships and the phenomena which follow from them, empirical information on force and interaction constants is required before polyiodide structural deductions can be made. Model compounds of known structure can provide such data. Figure 4A shows a solution resonance Raman spectrum of I_2; the intense stretching fundamental at 209 cm^{-1} is observed along with the characteristic[47] overtone progression. Figure 4B presents the spectrum of $(C_6H_5)_4As^+I_3^-$,[48] which contains isolated, symmetrical (equal I-I distances) I_3^- units.[48] As is empirically observed in all polyiodide resonance Raman spectra recorded to date,[10c] only the totally symmetric I-I stretching vibrations (for I_3^-, the in-phase stretching of the two oscillators) are appreciably enhanced with ν_0 = 4880-6471Å excitation. The actual I-I stretching frequency in I_3^- is the average of the symmetrically (118 cm^{-1}) and antisymmetrically (145cm^{-1}) coupled normal modes:[9,49] 132 cm^{-1}, which represents an appreciable lowering of the force constant from that in I_2. This feature illustrates an important point in understanding polyiodide electronic structure and vibrational spectra: molecular I_2 acts as a Lewis acid and coordination to Lewis bases, e.g. I^-, weakens the I-I bonding. Thus the I-I distance in I_2 is 2.72Å while in I_3^- it is near 2.92Å.[9] Molecular orbital calculations on I_3^- also show that the highest occupied molecular orbital has I-I anti-

bonding character.[50] When I_3^- units are placed in a linear chain [$((C_6H_5)$-$CONH_2)_2H^+I_3^-$][51] the electronic spectral visible maximum shifts somewhat,[10c,51] and I_3^- scattering is again observed (Figure 4C) but with a more pronounced overtone progression. The partially oxidized complexes $Ni(bqd)_2I_{0.5}$[7b,10a] and Ni(Pc)I[8] are examples of quasi one-dimensional stacked electrically conductive metallomacrocyclic systems with chains of I_3^- parallel to the stacking direction.[52] Examples are also known where crystal forces produce distortion of the I_3^- ions.[53] In CsI_3, I-I distances of 2.83(2) and 3.03(2)Å are observed,[48] and two resonance enhanced I-I stretching modes at 146 and 99 cm^{-1} (further split by small solid state effects[10c, 55]) are evident in the Raman spectrum (Figure 4D). Two other kinds of polyiodide structural motifs are also known. Crystallographically identifiable combinations of I_2 and I_3^- are observed in a number of materials such as $(Cs^+)_2(I_3^-)_2 \cdot I_2$,[55a] $(phenacetin)_2$-$H^+I_3^- \cdot I_2$,[55b] and $(C_2H_5)_4N^+I_3^- \cdot 2I_2$.[55c] The presence of <u>both</u> I_2 and I_3^- units are clearly evident,[10c] as exemplified by the spectrum of the phenacetin compound (Figure 4E). The I-I distance in the "I_2"[54] unit has lengthened to 2.748(2)Å which is reflected in the lower "I_2" νI-I frequency of 185cm^{-1}; the "I_3^-" totally symmetric stretch occurs at 119 cm^{-1}. The dotted lines in the structural drawing of Figure 4E represent relatively long I-I distances of 3.550(2)Å. A very weak emission at 160 cm^{-1} may evidence slight distortion of the I_3^- moiety. The bands at frequencies above 200 cm^{-1} can be assigned to overtone and combination bands of the above modes; this assures that the I_3^- and I_2 oscillators are in close proximity and that the

observed scattering pattern does not arise from a mixture of different compounds. Completely analogous spectra are observed for the other two $I_2 + I_3^-$ model compounds discussed above,[10c] with the only difference being that the distorted (I-I = 2.84 and 3.00Å) I_3^- units in Cs_2I_8[55a] give rise to a strong band at 150 cm^{-1} in addition to one at 105 cm^{-1}. This is completely analogous to the above mentioned situation in CsI_3. Examples have also been reported where I^- is symmetrically bound to two I_2 units. This species can be considered as the I_5^- ion and both linear [(trimesic acid · $H_2O)_{10} \cdot H^+I_5^-$][32] and bent $[(CH_3)_4N^+I_5^-]$[56] cases have been identified. The resonance Raman spectrum of the trimesic acid compound, which has chains of linear I_5^-, is illustrated in Figure 4F. The "I_2"[54] I-I stretching frequency of 160 cm^{-1} suggests that the I^- must now distribute electron density between two Lewis acid I_2 units and that the attendant lowering of the I-I force constant is not as great as in I_3^-. The reported[56] I_2 I-I distance of 2.74Å is in accord with this. The weak scattering at 107 cm^{-1} may be due to symmetric stretching which is predominantly $I_2 \leftarrow \bar{I} \rightarrow I_2$ in character;[57] the I--I distance is 3.24Å.[32] The selection rules for $D_{\infty h}$ I_5^- also predict a Raman-active π_g bending mode, which may occur at even lower frequency. The spacing between I_5^- units in this structure is 3.50Å. In summary, results for the various model compounds discussed form the basis for the Raman characterization of polyiodide structure in the $M(dpg)_2I$ series. The polyiodide spectra observed are generally rather insensitive in pattern to the laser exciting frequency (ν_0 = 4880 - 6471Å),[10b,c] and this is in agreement with the substantial breadth of most polyiodide solid state electronic

spectra.[10c,51] This situation will be illustrated in a later section (vide infra). In most cases the polyiodide electronic spectra consist of a number of severely overlapped transitions which have not been assigned with certainty.[58] The electronic transitions associated with large resonance Raman enhancement no doubt involve a significant structural change in going to the excited electronic state.[45]

Resonance Raman spectra of solid $Ni(dpg)_2$, $Ni(dpg)_2I$, $Pd(dpg)_2$, and $Pd(dpg)_2I$ are shown in Figure 5 and numerical data are presented in Table VII. Discussion of the optical spectra is deferred to the following section. Both iodides feature strong Raman scattering at 161 cm^{-1} and a weaker transition at ca. 107 cm^{-1}; overtone and combinations of these emissions are observed at ca. 210w(2 x 107), 268mw(161+107), and 324mw(2x161)cm^{-1}. That these transitions are assignable to a polyiodide and not to $M(dpg)_2$ units is supported by the observation that the analogous (and isostructural[14d]) $M(dpg)_2Br$ materials exhibit resonance enhanced scattering at energies assignable to polybromide species, but only weak scattering in the $M(dpg)_2I$ region(156 cm^{-1}).[59] Thus, the resonance-enhanced transitions at 161 and 107 cm^{-1} clearly arise from the polyiodide constituent. From the foregoing discussion two assignments seem most reasonable: a highly distorted I_3^- or an I_5^- moiety. As can be seen below, the same

$$I - I \text{-----} I^- \qquad\qquad I - I \text{---} \bar{I} \text{---} I - I$$

chromophore is present in each structure. Although a highly distorted I_3^- was at first considered a distinct possibility,[7c,d] that such

an extreme distortion should take place in the non-polar channels of the $M(dpg)_2$ crystal structure is not clear and not physically realistic.[53] Furthermore, such a degree of distortion is not evident in the Raman spectra of any model compound examined to date.[10c] On the other hand, the correspondence between the $M(dpg)_2I$ Raman spectra and those of the I_5^- chain model compound (trimesic acid$\cdot H_2O)_{10}\cdot H^+I_5^-$ (Figure 4) is strikingly close and argues persuasively for I_5^- as the predominant species. The band at 107 cm^{-1} in the $M(dpg)_2I$ spectra is, by analogy to the trimesic acid pentaiodide results, also attributable to I_5^-. There is no evidence for free I_2 in the Raman spectra. In addition to these results, it will also be seen that the fully refined I-129 Mössbauer spectra and the optical spectra are in good agreement with the I_5^- formulation. Efforts to obtain further vibrational spectroscopic information on the $M(dpg)_2I$ polyiodide component with far infrared techniques were unsuccessful. Comparison of spectra for the $M(dpg)_2$, $M(dpg)_2I$, and $M(dpg)_2Br$ compounds (see Experimental Section for data) revealed no significant absorption which could be assigned to an infrared-active I-I stretching transition;[9,49] these bands are apparently obscured by intense $M(dpg)_2$-centered normal modes.

The Raman spectra of both $M(dpg)_2$ and $M(dpg)_2I$ materials reveal weak bands at energies above 400 cm^{-1} (see Table VII for data), which are too narrow to be polyiodide overtone or combination bands. Furthermore, the band positions are sensitive to the nature of M. We assign these emissions to vibrations within the $M(dpg)_2$ and $M(dpg)_2^{+0.2}$ units. Interestingly, in accord with the crystallographic data, there is no evidence for discrete $M(dpg)_2$ units in the $M(dpg)_2I$ materials (i.e., trapped valency). When the

iodinated species are heated, iodine loss is accompanied by diminution of the $M(dpg)_2^{+0.2}$ "markers" and growth of the $M(dpg)_2$ "markers"; no spectra of intermediate species are observed. The internal coordinate changes associated with these bands are presumably analogous to the resonance enhanced metal-ligand or metal-influenced ligand vibrations observed for porphyrins[45, 60] and other metallomacrocycles.[46b, 61]

Iodine-129 Mössbauer Studies

Recoilless 27.7 keV nuclear resonant absorption spectroscopy between the $I_{ground} = 7/2$ and $I_{excited} = 5/2$ nuclear levels of iodine-129 is an established physical method for investigating structure and bonding in iodine containing materials.[62] For characterizing polyiodides, it is a useful supplement to resonance Raman spectroscopy since it can readily identify I^- (a spherically symmetrical electric field gradient about the iodine nucleus gives rise to zero quadrupole splitting).[7, 10] In addition, iodine-129 Mössbauer spectroscopy can be used for quantitative evaluation of relative site populations.[10, 62] The observed spectrum will be a superposition of the quadrupole patterns of the dissimilar iodine atoms in proportion to the respective populations. This ability to evaluate site populations is important in cases where resonance Raman techniques have not been sufficiently calibrated for quantitative assessments or where it is believed that unusual or previously unknown kinds of polyiodides are present. The distorted I_3^- versus I_5^- question discussed above, was part of the motivation for the present study.

Samples of $Ni(dpg)_2{}^{129}I$ and $Pd(dpg)_2{}^{129}I$ were prepared as described in the Experimental Section. Mössbauer spectra, obtained at 4°K, are shown

in Figure 6, along with computer generated theoretical spectra for the best fit to the data (see Experimental Section for details of this procedure). It will be seen that the data are in best agreement with an essentially $D_{\infty h}$ I_5^- species. For comparison, we also present the spectrum[10b] of the I_5^- chain compound (trimesic acid · $H_2O)_3 \cdot H^{+129}I_5^-$.[32] Stick spectra showing the quadrupole patterns for the three inequivalent iodine sites in $Ni(dpg)_2I$ are presented in the same figure. Numerical values of the parameters obtained from the spectral fitting procedure with their estimated standard deviations are given in Table VIII. The isomer shift and quadrupole coupling constants for corresponding sites in the three compounds are, within experimental error, very similar. Values of these parameters[63] are compared with those for symmetrical[64a,b] and distorted[64b,c] I_3^- in the scheme below.

δ(mm/sec)	0.25	1.48	0.25	0.12	1.15	-0.12
	I ——	I ——	I	I ——	I ------	I
$e^2q^{129}Q$(MHz)	-808	-1725	-808	-1041	-1782	-637
Relative site population	1.00	1.23	1.00			
	$[RuCp_2{}^{129}I]^{129}I_3$[64a,b]			$Cs^{129}I_3$[64b,c]		

δ(mm/sec)	0.52	1.20	0.18	1.20	0.52
	I ——	I ----	I ----	I ——	I
$e^2q^{129}Q$(MHz)	-1331	-1764	-880	-1764	-1331
Relative site population	1.00	1.02	1.00	1.02	1.00
	$M(dpg)_2{}^{129}I$[63]				

The above assignment of δ and e^2qQ to particular sites in I_5^- is that most consistent with bonding arguments (vide infra). It is also apparent from the values of the refined Mössbauer parameters in Table VIII that iodine

site populations in the $M(dpg)_2I$ materials are known with good but not as great a precision as δ and e^2qQ. For this reason a number of experiments were conducted to determine to what degree the populations given in Table VII were the most accurate representation of the proportions of possible sites present and what choices of polyiodides could be clearly rejected. In an attempt to fit the data to two inequivalent iodine sites, relative populations were constrained to 1:1 and to 1:2 (symmetrical I_3^-). This resulted in a marked deterioration of the goodness of fit parameter Misfit (see Experimental Section) from the values shown in Table VIII. This was true regardless of the choice of δ, e^2qQ, and linewidth. Similarly, fitting the data to three inequivalent iodine sites with relative site population 1:1:1 (unsymmetrical I_3^-) resulted in very poor agreement between experimental and calculated spectra for a wide range of reasonable δ, e^2qQ, and linewidth values. On the other hand, constraining the relative populations for three inequivalent iodine sites to 2:2:1 (e.g. symmetrical I_5^-) produced little change in the value of Misfit when compared with a three-site fit with no constraints on the relative populations. Thus, we conclude from the I-129 Mössbauer spectroscopy, as we concluded from resonance Raman spectroscopy that the predominant iodine-containing species in $Ni(dpg)_2I$ and $Pd(dpg)_2I$ is I_5^-.

On the basis of the present study, no extraneous iodine-containing species could be detected in the crystalline $M(dpg)_2{}^{129}I$ materials. It. is, however, worth considering to what level of contamination other iodine-containing species might be present but remain undetected, by I-129 Mössbauer spectroscopy. Based on known parameters[62] for I^-

(δ=-0.51 mm/sec, $e^2q^{129}Q$ = 0.00 MHz) and for I_2 in frozen hexane solution (δ = +0.98 mm/sec, $e^2q^{129}Q$ = -1586 MHz), we estimate that these species can be present to no greater than ca. 5 and 3 mole percent, respectively. The possibility that small amounts of either symmetrical or distorted I_3^- are present was also considered. It can be seen from published isomer shift and quadrupole coupling constants for triiodides[62,64] that many of the observed transitions will overlap with the I_5^- transitions, so that the maximum level of I_3^- impurities present can only be estimated from the relative site populations. Although we have found no direct evidence for any significant amount of I_3^-, symmetrical or distorted, we estimate that less than 5 molecule percent I_3^- impurity would be undectectable.

Examination of the isomer shift and quadrupole coupling constants for the I_5^- species yields information on charge distribution and bonding which can be meaningfully compared with results obtained for symmetrical and unsymmetrical I_3^-. Using a Townes-Dailey approach[65] as summarized by Ruby and Shenoy,[65c] the iodine-129 isomer shift versus ZnTe can be expressed as a function of the number of 5s electron holes, h_s, and the number of 5p electron holes, h_p (equation (7)).

$$\delta = -9.2h_s + 1.50h_p - 0.54 \text{ (mm/sec)} \qquad (7)$$

Alternatively, the effective 5p electron imbalance, U_p, can be calculated directly (equation (8)) from the ratio of the

$$U_p = -e^2q_{mol}{}^{129}Q/e^2q_{atom}{}^{129}Q \qquad (8)$$

experimental value of the nuclear quadrupole coupling constant in the molecule under examination ($e^2q_{mol}{}^{129}Q$) to that of atomic iodine ($e^2q_{atom}{}^{129}Q$ = 1670 MHz, U_p = 1). Here U_p is defined in equation (9) in terms of the 5p electron populations in the three Cartesian spatial directions.

$$U_p = -U_z + \tfrac{1}{2}(U_x + U_y) \qquad (9)$$

For axial symmetry, the asymmetry parameter is zero and $U_x = U_y$.[62,66] Prior studies[62,64] have shown that in polyiodides such as I_2 and I_3^- the bonding largely if not exclusively involves the p_z orbitals;[62,64a] hence it can be assumed that $h_s \approx 0$ and $U_x = U_y \approx 2$. From equations (7) - (9) it can be seen that U_p, U_z, and thus the approximate charges on the iodine atoms can be calculated from two independent approaches.[66] The agreement of these two methods serves as an additional check on the quality of the data and the internal consistency of the parameter values obtained.[66c] The scheme below sets out the calculated charge distributions (equation (7)) and equation (8)) for symmetrical I_3^-, distorted I_3^-, and I_5^-[67]. The charge distribution results based upon

from δ	-0.47	+0.35(+0.25)[68]	-0.47	-0.56	+0.13	-0.72
	I	—— I ——	I	I	—— I -------	I
from e^2qQ	-0.49	+0.07	-0.49	-0.35	+0.11	-0.60

from δ	-0.29	+0.17	-0.58	+0.17	-0.29
	I ——	I ------	I	------ I ——	I
from e^2qQ	-0.20	+0.10	-0.44	+0.10	-0.20

quadrupole splitting data are probably slightly more reliable in most cases since the probable error in a large e^2qQ value typically represents a smaller percentage of the derived charge distribution. In terms of electronic structure, the results of the above calculations reveal that distorting the I_3^- ion is equivalent, in a first order approximation, to pulling an I^- away from I_2. That is, the resulting values of isomer shifts and quadrupole coupling constants tend toward I_2 and I^- in that the charges on the "departing" iodide becomes more negative while the charge on the iodine atoms in the emerging I_2 unit tend toward neutrality. The I_5^- molecule exhibits a similar pattern in the "I_2" fragments, i.e., the charge distribution is more nearly equal and the charge concentration less negative than in I_3^-. Interestingly, the central iodine atom in I_5^- does not possess as great a negative charge as the "departing" iodine atom in distorted I_3^-. This can be rationalized by the observation mentioned in the Raman discussion, that the "I^-" in I_5^- must share its electron density with two I_2 Lewis acid units. Reversing the assignment of the two highly populated sites in I_5^- results in an ion with positive charge on the two outer iodine atoms and negative charge on the three inner iodine atoms. In terms of chemical bonding and the foregoing discussion, this must be regarded as highly unlikely.

Electronic Spectra

Electronic absorption spectra of the $M(dpg)_2$ and $M(dpg)_2I$ materials, M = Ni and Pd, as Nujol mulls are presented in Figure 7A-D. These data as well as those for chloroform solutions are compiled in Table IX. The spectral features of $Pd(dpg)_2$ and $Ni(dpg)_2$ are closely analogous to those of other stacked d^8 palladium and nickel bisglyoximates.[69] There is also a close similarity in transition energies. Furthermore, the two lowest energy spectral transitions in the polycrystalline $M(dpg)_2$ samples are not observed in solution, again a distinctive characteristic of stacked bisglyoximate systems. Thus, the 515 nm absorption in $Ni(dpg)_2$ and the 445 nm absorption in $Pd(dpg)_2$ can be correlated with stacked glyoximate transitions[69] which are found to be polarized parallel to the chain direction in single crystal studies[69] and which ligand[70] and metal[70b, 71] substitution as well as pressure dependence[69b, 72] reveal to be highly sensitive to the intrastack metal-metal separation. These spectral features have been assigned to intramolecular $nd_{z^2} \rightarrow (n + 1)p_z$ transitions which borrow intensity from intermolecular metal $\longrightarrow$ metal charge transfer transitions.[69] In addition, the $(n + 1)p_z$ orbitals may be mixed with ligand π^* molecular orbitals.[69a] The next highest energy bands (435 nm for $Ni(dpg)_2$ and 365 nm for $Pd(dpg)_2$) are analogous to those assigned to metal-to-ligand ($d\pi \rightarrow \pi^*$) charge transfer absorptions.[69] The energies of such transitions are generally rather insensitive to metal-metal separation.[69] Upon halogenation

of the $M(dpg)_2$ materials, several noteworthy changes occur in the spectra (Figure 7A and C). A very broad transition, centered at ca. 675 nm, appears. Though such a transition might, a priori, be associated with mixed valency,[6b,73] comparison with the spectrum of the model I_5^- chain compound, (trimesic acid · $H_2O)_{10}$ · $H^+I_5^-$, provides a persuasive argument for assignment as a polyiodide transition. Indeed, polyiodide electronic spectra are quite distinctive and can even be employed for qualitative structural assignments.[10c,74] Thus, broad absorptions centered near 700 nm are typically found in I_5^- chain compounds. The other spectral feature which is evident upon $M(dpg)_2$ halogenation is the disappearance or weakening of the long wavelength $nd_{z^2} \rightarrow (n+1)p_z$ transitions and the appearance of a new band at 566 nm in $Ni(dpg)_2I$ and at 505 nm in $Pd(dpg)_2I$. In the absence of polarized single crystal data[75] all that can be remarked about the origin of these transitions is that the data are consistent with an expected red shift of the aforementioned $nd_{z^2} \rightarrow (n+1)p_z$ transitions on contraction of the metal-metal separation. The energy shifts for the nickel and palladium absorptions are comparable, i.e., 9% and 12% respectively, as are the contractions in metal-metal distances, i.e., 3.55 → 3.27 Å and 3.52 → 3.26 Å, respectively.

X-Ray Photoelectron Spectra

XPS[76] data can provide useful information on the electronic structure of mixed valence materials[77] when they are acquired[78] and interpreted with care[79]. In the present case, such data offered the possibility of assessing to what

degree the fractional oxidation states in $Ni(dpg)_2I$ and $Pd(dpg)_2I$ might be localized, i. e., to what degree discrete sites such as Ni^{+2} and Ni^{+3} or Ni^{+4} might be present (Type I or Type II mixed valency).[73] The rapid XPS timescale (ca. 10^{-18} sec.) is particularly advantageous for this purpose.[76] In the case of a Type III system, XPS offered the possibility of detecting major changes in charge distribution accompanying partial oxidation. Since XPS is a surface technique, the presence of iodine was continuously monitored during the $M(dpg)_2I$ studies to ensure that the uniodinated species were not being produced by the high vacuum or X-ray bombardment. In Figure 8 are presented $2p_{3/2}$ spectra of $Ni(dpg)_2$ and $Ni(dpg)_2I$, and $3d_{5/2}$, $3d_{3/2}$ spectra of $Pd(dpg)_2$ and $Pd(dpg)_2I$; data are set out in Table X. The important observations to be made are that the binding energies and linewidths of corresponding $M(dpg)_2$ and $M(dpg)_2I$ materials, while in good agreement with literature data for nickel[76,80] and palladium[76,81] complexes, do not differ significantly from each other. There is no evidence of trapped valence or of appreciable change in metal atom charge in the halogenated materials. The absence of detectable "shake-up" satellites (core ionization plus molecular electronic excitation) in the nickel spectra is in agreement with the diamagnetism and square-planar coordination geometry.[80] Attempts to clean the surface of the iodinated materials by argon ion etching resulted in halogen loss. Element loss resulting from argon ion bombardment has been observed before.[82]

Electrical Conductivity

Single crystal measurements of the electrical conductivities of the $M(dpg)_2$ and $M(dpg)_2I$ compounds were performed as a function of temperature by the standard four-probe technique (see Experimental Section for details). The needle-like morphology of the crystals precluded measurements in any direction other than parallel to the molecular stacking direction.

In Figures 9 and 10 are shown plots of representative conductivity data for $Ni(dpg)_2I$ and $Pd(dpg)_2I$. These as well as related data are summarized in Table XI. The range of conductivity is given at 300°K for all samples examined and is compared with the values for the corresponding unoxidized materials. In the case of the unoxidized samples, the values presented are an upper limit imposed by the sensitivity of the instrumentation and the geometry of the available samples; the actual conductivities may be one or more orders of magnitude less than 10^{-9} $(\Omega\text{-cm})^{-1}$. Also compared in Table XI are the dc and low frequency ac conductivities measured on the same $M(dpg)_2I$ specimens. The excellent agreement obtained indicates a minimum of undesirable electrode-contact effects in the conductivity measurements.

As can be readily recognized from Figures 9 and 10, the data adhere closely to a linear dependence of $\ln\sigma$ vs. $1/T$ for the temperature range investigated. This behavior suggests that the thermal activation model of eq (10)

$$\sigma = \sigma_0 e^{-\Delta/kT} \qquad (10)$$

where there is a single activation energy, Δ, is the most appropriate description. In Table XI the average activation energy is presented for each material as obtained from a least-squares fit of the data to eq (10). The extent of variation for the values presented represents the largest deviation from the average for all samples shown. Especially for $Ni(dpg)_2I$, all samples are remarkably similar in the slope of the $\ln\sigma$ vs. $1/T$ plot.

The data presented in Figures 9 and 10 were found to be reproducible when taken in order of either increasing or decreasing temperature. Although a slight fall-off in the slope of the $\ln\sigma$ vs. $1/T$ plots may occur at the highest temperatures shown,[84] attempts to reach higher temperatures were thwarted by sample decomposition. In these cases, returning the sample to room temperature did not restore the conductivity to its original value.

Two important features are obvious upon viewing the conductivity data. First, the iodination has brought about a very large increase in the facility of charge transport (ca. 10^7-10^8). Although a similar effect has been noted for other metallomacrocycle systems upon halogenation,[7a, 7b, 8a, d] the bis(diphenylglyoximates) represent the first case where the only feature of the donor crystal structure variable to change upon halogenation is the interplanar spacing. The second feature of note in the $M(dpg)_2I$ data is the dependence of the conductivity on the identity of M. The dependence is small, with $Ni(dpg)_2I$ being slightly more conductive. This result is surprising in

view of the fact that the metal-metal distances are essentially equal on proceeding from nickel to palladium and the metal ionic radius increases by ca. 0.16Å.[38] The effect of interplanar spacing on the charge transport characteristics of partially oxidized bis(glyoximates) will be explored further in the discussion of bis(benzoquinonedioximate) systems.[7b] The relative insensitivity of conductivity to the metal has been noted in other highly conjugated, partially oxidized metal-macrocycle materials.[7a, 8a, d]

A significant question in considering the conductivity increase brought about by $M(dpg)_2$ iodination, is whether the charge transport path may not involve the stacked array of partially oxidized $M(dpg)_2$ units, but rather the chains of iodine atoms (as I_5^- units). Elemental iodine is a wide gap semiconductor which becomes metallic under sufficient pressure.[85] To explore this matter further, conductivity studies were undertaken on integral oxidation state materials with polyiodide chains. Polycrystalline samples of (trimesic acid$\cdot H_2O)_{10}H^+I_5^-$ (having I_5^- chains[32]) exhibited electrical conductivity less than 10^{-7} $(\Omega - cm)^{-1}$, while samples of (benzamide)$_2$-$H^+I_3^-$ (having I_3^- chains[51]) were comparable in low conductivity: less than 10^{-8} $(\Omega - cm)^{-1}$.[86] Experience indicates that for typical quasi one-dimensional materials, polycrystalline samples will be ca. 10^{-2} less conductive than single crystals measured along the chain direction.[8a,b,87] Further evidence that the polyiodide chains play at most a minor role in charge transport is provided by results on the analogous brominated compounds. Both polycrystalline and single crystal samples of the

$M(dpg)_2Br$ materials display conductivities which are, within experimental error, identical to those of the analogous $M(dpg)_2I$ materials.[59] This demonstrates an insensitivity of the transport properties to the identity of the halogen.

It is of interest to compare the facility of charge transport in the $M(dpg)_2I$ systems with that of other low dimensional materials. To take account of differences in crystal structures, it is most meaningful to compare the mean free paths, L, which describe the average distance travelled by a charge carrier between scattering occurrences. From one-electron band theory, the dc conductivity in the chain direction can be related to the mean free path by eq. (11),[86, 88] where

$$L = \frac{\pi\hbar A\sigma}{2e^2N} \qquad (11)$$

A is the stack cross-sectional area and N is the number of conducting chains per cross-sectional area. The mean free paths for the $M(dpg)_2I$ charge carriers are compared with those of several other stacked materials in Table XII. The parameters for the partially oxidized bisdiphenylglyoximates are comparable with those for "intermediate-conductivity" salts of TCNQ(tetracyanoquinodimethane).[89] The latter materials also exhibit temperature-dependent conductivity which follows eq. (10).[89]

The theoretical reasons for the observed temperature dependence of the electrical conductivity in quasi one-dimensional stacked organic and metal-organic materials have been the subject of considerable

discussion. For the $M(dpg)_2I$ compounds, which exhibit activated behavior with at most only minor levelling-off of the conductivity at highest attainable temperatures, either of two currently proposed models appears to be applicable. Phonon-assisted hopping has been discussed for anisotropic systems in which the electronic states near the Fermi level are localized owing to static disorder.[87c, 90] The lack of registry between polyiodide chains detected in the diffraction study is the most obvious structural disorder in the $M(dpg)_2I$ system. For the regime above the very lowest temperatures (where variable-range hopping occurs) this model predicts activated charge transport behavior, i.e., eq. (10) is obeyed.

At higher temperatures it is proposed that the electron-phonon interaction becomes stronger than the potential causing the localization, and the activated behavior is no longer observed. This higher temperature range is presumably beyond that which is practicable for the $M(dpg)_2I$ materials. Alternatively, a description has been put forward based on the observation that the conductivity of a number of low-dimensional materials can be fit to eq. (12).[91] Here

$$\sigma = \sigma_0 T^{-\alpha} e^{-\Delta/kT} \qquad (12)$$

α is a sample-dependent constant in the range of 3 to 4. It has been proposed that most of the electronic states in these materials are only weakly localized and that a band model with a gap (possibly a Mott-Hubbard gap or one associated with disorder-induced localization of states at the

band edges) of 2Δ is applicable. The exponential term in eq. (12) reflects an activated carrier concentration. The factor $T^{-\alpha}$ arises from a marked temperature dependence of the carrier mobility and can be related to coupling with molecular vibrations. In practice, a number of materials which conform to eq. (12) exhibit a nearly linear region in the log σ vs. 1/T plot (although pronounced downward curvature is seen at higher temperatures). From the above discussion it can be seen that the relatively linear log σ vs. 1/T behavior of the $M(dpg)_2I$ materials is compatible with either conductivity model. A serious question regarding the hopping picture is whether the disordered iodine chains could provide sufficient driving force for localization of the electronic wave functions in the $M(dpg)_2$ columns. A serious question with regard to the band model concerns the origin of the apparent gap. For the present case with 90% filled band, it seems unlikely to be Mott-Hubbard in origin.[91b]

CONCLUSIONS

The results of this study demonstrate conclusively that $M(dpg)_2I$ compounds, M = Ni, Pd, contain the $M(dpg)_2$ units in formal fractional oxidation states, ca. +0.2. The accuracy of this number is limited primarily by the accuracy to which the stoichiometry of the compound is known and by the possible presence of small amounts of undetected iodine-containing species. A reasonable estimate of uncertainty is ±0.04 charge units. Thus, it is seen that the diffuse x-ray scattering, resonance Raman, and iodine-129 Mössbauer techniques are powerful complementary methods for polyiodide structure identification, and hence for direct measurement of charge distribution in mixed valence lattices. Judging from the $M(dpg)_2$ and other metallomacrocycle results[7,8], the iodine oxidation procedure appears to have some efficacy in the synthesis of mixed valence lattices, and in the present case results both in shortening of the metal-metal distance (ca. 0.27 Å) and in dramatically increasing the c axis conductivity (ca. 10^7-10^8). Whether the charge carriers are transported through the chain of metal atoms as is likely in KCP ($K_2Pt(CN)_4Br_{0.3}\cdot 3H_2O$)[3b] or through the π systems of the ligand columns as in numerous organic conductors, has not been resolved. The large intermetal distances in the present case, i.e., 3.223(3)Å (3.25Å for Pd[14d]) vs. 2.89 Å in KCP[92], and the relative insensitivity of the conductivity to the metal argue for the latter situation.[93]

It is reasonable to inquire whether chemical modification of the metal bisglyoximate core so as to allow greater conjugation and closer interplanar spacing will affect the degree of partial oxidation, transport properties, etc. This question is explored further in the accompanying article.[7b]

ACKNOWLEDGMENTS

We thank Mr. C. B. Cooper for assistance with the 8 °K Raman measurement. We are indebted to Prof. J. B. Cohen for generously making his facilities for diffuse x-ray measurements available to us. This work was generously supported under the NSF-MRL program through the Materials Research Center of Northwestern University (grant DMR76-80847), by the Office of Naval Research (grant N00014-77-C-0231 to T. J. M.), the Department of Energy (S. L. R.), and the National Science Foundation (grant CHE76-10335 to J. A. I.)

Supplementary materials available: A listing of structure factor tables. Ordering information is given on any current masthead page.

References

(1) a. Department of Chemistry and the Materials Research Center, Northwestern University.
b. Department of Electrical Engineering and the Materials Research Center, Northwestern University.
c. Physics Division, Argonne National Laboratory.
d. Thesis parts appointee, Argonne National Laboratory.

(2) a. Fellow of the Alfred P. Sloan Foundation
b. Camille and Henry Dreyfus Teacher-Scholar.

(3) a. Keller, H.J., ed. Chemistry and Physics of One-Dimensional Metals, Plenum Press, New York, 1977.
b. Miller, J.S.; Epstein, A.J. Prog. Inorg. Chem., 1976, 20, 1-151.
c. Keller, H.J., ed. Low Dimensional Cooperative Phenomena, Plenum Press, N.Y., 1975.
d. Soos, Z.G.; Klein, in Molecular Associations, Foster, R., ed., Academic Press, N.Y., 1975, chapt. 1.
e. Masuda, K.; Silver, M. Charge and Energy Transfer in Organic Semiconductors, Plenum Press, N.Y., 1974.
f. Interrante, L.V. Extended Interactions Between Metal Ions in Transition Metal Complexes, ACS Symposium Series, 5, 1974.
g. Zeller, H. R. Festkörperprobleme, 1973, 13, 31-58.

(4) a. Bloch, A.N.; Cowan, D. O.; Bechgaard, K.; Pyle, R.E.; Banks, R.H. Phys. Rev. Letters, 1975, 34, 1561-1564.
b. Ashwell, G.J.; Eley, D. D.; Willis, M.R. Nature, 1976, 259, 201-202.
c. Isett, L. C.; Perez-Albuerne, E. A. Solid State Comm., 1977, 21, 433—435.
d. Bechgaard, K.; Jacobsen, C.S.; Anderson, N.H. Solid State Comm. 1978, 25, 875-879.

(5) a. Garito, A. F.; Heeger, A.J. Accounts Chem. Res., 1974, 7, 232-240.
b. Haddon, R. C. Nature, 1975, 256, 394-396.
c. Soos, Z. G. Ann. Rev. Phys. Chem., 1974, 25, 121-153.

(6) a. Pouget, J.P.; Khanna, S. K.; Denoyer, F.; Comes, R.; Garito, A.F.; Heeger, A.J. Phys. Rev. Letters, 1976, 37, 437-440.
b. Torrance, J. B.; Scott, B. A.; Kaufman, F. B. Solid State Comm., 1975, 17, 1369-1373.
c. Butler, M. A.; Wudl, F.; Soos, Z. G. Phys. Rev., 1975, B, 12, 4708-4719.
d. LaPlaca, S.J.; Corfield, P.W.R.; Thomas, R.; Scott, B.A. Solid State Comm., 1975, 17, 635-638.
e. Coppens, P. Phys. Rev. Letters, 1975, 35, 98-100.

(6) f. Torrance, J. B. Lecture Notes in Physics, 1977, 65, 453-467.
g. For apparent exceptions to this generalization, involving second and third row transition metal ions, see: Reise, A. H., Jr.; Hagley, V. S.; Petersen, S. W. J. Amer. Chem. Soc., 1977, 99, 4184-4186. Gordon, J. G., II; Williams, R.; Hsu, C. H.; Cuellar, E.; Samson, S.; Hadek, V.; Somoano, R. N. Y. Acad. Sci. Conf. on Synthesis and Properties of Low-Dimensional Materials, N. Y., June, 1977, Abstract 37; Megnamisi-Bélombé, M. J. Solid State Chem., 1977, 22, 151-156.

(7) a. Marks, T. J. Ann. N. Y. Acad. Sci., in press.
b. Brown, L. D.; Kalina, D. W.; McClure, M. S.; Ruby, S. L.; Schultz, S.; Ibers, J. A.; Kannewurf, C. R.; Marks, T. J. submitted for publication.
c. Gleizes, A.; Marks, T. J.; Ibers, J. A. J. Amer. Chem. Soc., 1975, 97, 3545-3546.
d. Marks, T. J.; Gleizes, A.; Ibers, J. A. Abstracts, 170th Meeting of the American Chemical Society, Chicago, Illinois, August, 1975, INOR 54

(8) a. Petersen, J. L.; Schramm, C. S.; Stojakovic, D. R.; Hoffman, B. M.; Marks, T. J. J. Amer. Chem. Soc., 1977, 99, 286-288.
b. Schramm, C. S.; Stojakovic, D. R.; Hoffman, B. M.; Marks, T. J. Science, 1978, 200, 47-48.
c. Peterson, J. L.; Schramm, C. S.; Scaringe, R. P.; Stojakovic, D. R.; Hoffman, B. M.; Ibers, J. A.; Marks, T. J., manuscript in preparation.
d. Lin, L.-S.; Marks, T. J., manuscript in preparation.

(9) Popov, A. I. MTP International Review of Science, Inorganic Chemistry, Series One, 1972, Gutmann, V., Ed., University Park Press, Vol. 3 Baltimore, MD, Chapt. 2.

(10) a. Marks, T. J.; Webster, D. F.; Ruby, S. L.; Schultz, S. J. Chem. Soc. Chem. Comm., 1976, 444-445.
b. Teitelbaum, R. C.; Ruby, S. L.; Marks, T. J. J. Amer. Chem. Soc. 1978, 100, 3215-3217.
c. Kalina, D. W.; Stojakovic, D. R.; Teitelbaum, R. C.; Marks, T. J., manuscript in preparation.

(11) Williams. D. E.; Wohlauer, G.; Rundle, R. E. J. Amer. Chem. Soc., 1959, 81, 755-756.

(12) Edelman, L. E. J. Amer. Chem. Soc., 1950, 72, 5765-5766.

(13) Underhill, A. E.; Watkins, D. M.; Pethig, R. Inorg. Nucl. Chem. Letters, 1973, 9, 1269-1273.

(14) a. Miller, J. S.; Griffiths, C. H. J. Amer. Chem. Soc., 1977, 99, 749-755.
b. Mehne, L. F.; Wayland, B. B. Inorg. Chem., 1975, 14, 881-885.
c. Keller, H. J.; Seibold, K. J. Amer. Chem. Soc., 1971, 93, 1309-1310.
d. Foust, A. S.; Soderberg, R., J. Amer. Chem. Soc., 1967, 89, 5507-5508.

(15) a. Foster, R. Organic Charge-Transfer Complexes, 1969, Academic Press, New York.
b. Mulliken, R. S.; Person, W. B. Molecular Complexes, 1969, Wiley-Interscience, New York.

(16) a. Barefield, E. K.; Mocella, M. T. J. Amer. Chem. Soc., 1975, 97, 4238-4246.
b. Lovecchio, F. V.; Gore, E. S.; Busch, D. H. J. Amer. Chem. Soc., 1974, 96, 3109-3118.
c. Dolphin, D.; Niem, T.; Felton, R. H.; Fujita, I. J. Amer. Chem. Soc., 1975, 5288-5290.
d. Lappin, A.G.; Murray, C.K.; Margerum, D.W. Inorg. Chem., 1978, 17, 1630-1634 and references therein.
e. Johnson, E. C.; Niem, T.; Dolphin, D. Can. J. Chem., 1978, 56, 1381-1388.

(17) Cooper, C. B. Ph.D. Thesis, Northwestern University, July, 1978.

(18) Ruby, S. L. Mössbauer Effect Methodology, 1973, 8, 263-276.

(19) The traditional goodness-of-fit parameter

$$\chi^2 = \sum_i^n |(\chi_i - \chi_{ic})/\Delta\chi_i|^2$$

gives satisfactorily small values for either a good model (the calculated values χ_{ic} agree well with the data χ_i) or for a poor experiment ($\Delta\chi_i$ is large).[18]

(20) Schafer, D. E.; Wudl, F.; Thomas, G. A.; Ferraris, J. P.; Cowan, D. D. Solid State Commun., 1974, 14, 347-351.

(21) We thank Dr. R. Bastasz for a copy of this program.

(22) Cowie, M.; Ibers, J. A. Inorg. Chem., 1976, 15, 552-557.

(23) Doedens, R. J.; Ibers, J. A. Inorg. Chem., 1967, 6, 204-210.

(24) The Northwestern absorption program. AGNOST, includes the Coppens-Leiserowitz-Rabinovitch logic for Gaussian integration. The diffractometer was run under the disc oriented Vanderbilt system (Lenhert, P. G. J. Appl. Cryst., 1975, 8, 568-570). Other programs used are described in ref. 22.

(25) For non-hydrogen atom scattering factors see: Cromer, D. T.; Waber, J. T. International Tables for X-ray Crystallography 1974, Vol IV, Kynoch Press, Birmingham, England, Table 2.2A. For hydrogen atoms see: Stewart, R. F.; Davidson, E. R.; Simpson, W. T. J. Chem. Phys. 1965, 42, 3175-3187.

(26) Cromer, D. T.; Liberman, D. J. Chem. Phys., 1970, 53, 1891-1898.

(27) Warren, B. E., X-ray Diffraction, Addison-Wesley, Reading, Mass., 1969, p. 35.

(28) Scaringe, R. P.; Ibers, J.A. unpublished results.

(29) See paragraph at end of paper regarding supplementary material.

(30) a. Endres, H.; Keller, H. J.; Megnamisi-Bélombé, M.; Moroni, W.; Pritzkow, H.; Weiss, J.; Comes, R. Acta Cryst., 1976, A32, 954-957.
b. Smith, D. L.; Luss, H. R., Acta. Cryst., 1977, B33, 1744-1749.
c. Huml, K. Acta Cryst., 1967, 22, 29-32.

(31) Beyeler, H. U. Phys. Rev. Lett., 1976, 37, 1557-1560.

(32) Chains of linear I_5^- ions are found in (trimesic acid$\cdot H_2O)_{10}H^+I_5^-$. See: Herbstein, F. H.; Kapon, M. Acta Cryst., 1972, A28, S74, and private communication to T.J.M.

(33) Endres, H.; Keller, H. J.; Moroni, W.; Weiss, J. Acta Cryst., 1975, B31, 2357-2358.

(34) Robertson, J. M.; Woodward, I. J. Chem. Soc., 1937, 219-220.

(35) a. Millar, M.; Holm. R. H. J. Amer. Chem. Soc., 1975, 97, 6052-6058.
b. Peng, S. -M.; Ibers, J. A.; Millar, M.; Holm, R. H. J. Amer. Chem. Soc., 1976, 98, 8037-8041.

(36) Peng, S. -M.; Goedken, V. L. J. Amer. Chem. Soc., 1976, 98, 8500-8510.

(37) Charlson, A. J.;. Stephens, F. S.; Vagg, R. S.; Watton, E. C. Inorg. Chim. Acta., 1977, 25, L51-L52.

(38)a. Handbook of Chemistry and Physics, 57th ed., Chemical Rubber Publishing Co., Cleveland, Ohio, 1976-1977, p. F-216.
b. Shannon, R. D.; Prewitt, T. T. Acta Cryst., 1969, B25, 925-930.

(39) Sacconi, L. Transition Metal Chem., 1968, 4, 199-298.

(40) Fleischer, E. B. J. Am. Chem. Soc., 1963, 85, 146-148.

(41) Hamor, T. A.; Caughey, W. S.; Hoard, J. L. J. Am, Chem. Soc., 1965, 87, 2305-2312.

(42)a. Meyer, E. F., Jr. Acta Cryst., 1972, B28, 2162-2167.

b. Cullen, D. L.; Meyer, E. F., Jr. J. Am. Chem. Soc., 1974, 96, 2095-2102.

(43) Dwyer, P. N.; Buchler, J. W.; Scheidt, W. R. J. Am. Chem. Soc., 1974, 96, 2789-2795.

(44) See, for example, Guinier, A. X-ray Diffraction in Crystals, Imperfect Crystals, and Amorphous Bodies, W. H. Freeman and Co., San Francisco, 1963, p. 154.

(45) a. Johnson, B. B.; Peticolas, W. L. Ann. Rev. Phys. Chem., 1976, 27, 465-491.
b. Warshel, A. Ann. Rev. Biophys. Bioeng., 1977, 6, 273-300.
c. Spiro, T. G. Chemical and Biochemical Applications of Lasers, Moore, C. B., ed., Academic Press, New York, 1974, chapt. 2.
d. Tang, J.; Albrecht, A. C. Raman Spectroscopy, Szymanski, H. A., ed., Plenum Press, New York, Vol. 2, Chapt. 2.

(46) a. Johnson, B. B.; Nafie, L. A.; Peticholas, W. L. Chem. Phys. 1977, 19, 303-311.
b. Nafie, L. A.; Pastor, R. W.; Dobrowiak, J. C.; Woodruff, W. H. J. Amer. Chem. Soc., 1976, 98, 8007-8014.
c. Stein, P.; Miskowski, V.; Woodruff, W. H.; Griffin, J. P.; Werner, K. G.; Gaber, B. P.; Spiro, T. G. J. Chem. Phys., 1976, 64, 2159-2167.
d. Mingardi, M.; Siebrand, W. J. Chem. Phys., 1975, 62, 1074-1085.

(47) Kiefer, W. Appl. Spectrosc., 1974, 28, 115-133.

(48) Runsink, J.; Swen-Walstra, S.; Migchelsen, T. Acta. Cryst., 1972, B28, 1331-1335.

(49) a. Maki, A. G.; Forneris, R. Spectrochim., Acta., 1967, 23A, 867-880, and references therein.
b. Haywood, G. C.; Hendra, P. J. Spectrochim. Acta., 1967, 23A 2309-2314.

(50) Gabes, W.; Nijman-Meester, M.A.M. Inorg. Chem., 1973, 12, 589-592.

(51) Reddy, J. M.; Knox, K.; Robin, M. B. J. Chem. Phys., 1964, 40, 1082-1089.

(52) A number of highly conductive organic materials display a similar structural motif of stacks and I_3^- chains. See references 30b, c, and Delhaes, P.; Cougrand, A.; Flandrois, S.; Chasseau, D.; Gaultier, J.; Hauw, C.; Dupuis, P. Lecture Notes in Physics, 1977, 65, 493-498.

(53) a. Brown, R.D.; Nunn, E. K. Austral. J. Chem., 1966, 19, 1567-1576.
b. Migchelsen, T.; Vos, A. Acta. Cryst., 1967, 22, 812-815.
c. Rundle, R.E. Acta Cryst., 1961, 14, 585-589.

(54) a. Correlation field effects are generally observed to be relatively small in polyiodides.[10c] For example, the factor group splitting in solid I_2 is only ca. 8 cm^{-1}.[55b]
b. Anderson, A.; Sun, R. S. Chem. Phys. Letters, 1970, 6, 611-616.

(55) a. Havinga, E. E.; Boswijk, K. H.; Wiebenga, E. H. Acta. Cryst 1954, 7, 487-490.
b. Herbstein, F. H.; Kapon, M. Nature(London), 1972, 239, 153-154.
c. Havinga, E. E.; Wiebenga, E. H. Acta Cryst., 1958, 11, 733-737.

(56) Hach, R. J.; Rundle, R. E. J. Amer. Chem. Soc., 1951, 73, 4321-4324.

(57) Since this normal mode has the same symmetry (A_{1g} under D_{2h}) as the 160 cm^{-1} mode, there is presumably some mixing of the vibrations.

(58) a. Gabes, W.; Stufkens, D. J. Spectrochim. Acta., 1974, 30A, 1835-1841, and references therein.
b. Robin, M. B. J. Chem. Phys., 1964, 40, 3369-3377.

(59) Kalina, D. W.; McClure, M. S.; Kannewurf, C.R.; Marks, T.J., manuscript in preparation.

(60) a. Sunder, S.; Mendelsohn, R.; Bernstein, H. J. J. Chem. Phys. 1975, 63, 573-580.
b. Friedman, J. M.; Hochstrasser, R. M. J. Amer. Chem. Soc., 1976, 98, 4043-4048
c. Shelnutt, J. A.; O'Shea, D. C.; Yu, N.-T.; Cheung, L.D.; Felton, R.H. J. Chem. Phys., 1976, 64, 1156-1165.

(61) Woodruff, W. M.; Pastor, R. W.; Dobrowiak, J. C. J. Amer. Chem. Soc., 1976, 98, 7999-8006.

(62) a. Gibb, T. C. Principles of Mössbuaer Spectroscopy, Chapman and Hall, London, 1976, Chapt. 4.2.
b. Bancroft, G. M.; Platt, R. H. Adv. Inorg. Chem. Radiochem., 1972, 15, 59-258.

(63) Data for $Ni(dpg)_2I$ and $Pd(dpg)_2I$ have been averaged.

(64) a. Potasek, M.J.; Debrunner, P. G.; Morrison, W. H., Jr.; Hendrickson, D.N. J. Chem. Phys., 1974, 60, 2203-2206.
b. Ehrlich, B. S.; Kaplan, M J. Chem. Phys., 1969, 51, 603-606
c. deWaard, H.; Ruby, S. L., unpublished results on Cs $^{129}I_3$.

(65) a. Lucken, E.A.C. Nuclear Quadrupole Coupling Constants, Academic Press, London, 1969, Chapt.
b. Dailey, B.P.; Townes, C.H. J. Chem. Phys., 1955, 23, 118-123
c. Ruby, S. L.; Shenoy, G.K. Mössbauer Isomer Shifts, Shenoy, G.K.; Wagner, F.E., Eds., North Holland, Amsterdam, 1978, chapt. 9b.

(66) a. Bukshpan, S.; Goldstein, C.; Sonnino, T.; May, L.; Pasternak, M. J. Chem. Phys., 1975, 62, 2606-2609.
b. deWaard, H. Mössbauer Effect Data Index, 1973, 447-494.
c. This means that for a similar class of compounds, there will be a linear relationship between δ and e^2qQ.

(67) That the sum of the charges on each ion does not equal -1.0 illustrates the crudeness of this approach.

(68) The charge on the central iodine atoms of the I_3^- groups in $Ru(C_5H_5)_2I^+I_3^-$ and $(C_5H_5CONH_2)_2H^+I_3^-$, calculated from the published isomer shifts, is not in optimal agreement, so both values are given.

(69) a. Anex, B.G. A.C.S. Symposium Series, 1974, 5, 276-300.
b. Hara, Y.; Shirotani, I.; Onodera, A. Solid State Comm., 1976, 19, 171-175.
c. Ohashi, Y.; Hanazaki, I.; Nagakura, S. Inorg. Chem., 1970, 9, 2551-2556.

(70) a. Anex, B.G.; Krist, F.K. J. Amer. Chem. Soc., 1967, 89, 6114-6125.
b. Banks, C. V.; Barnum, D.W. J. Amer. Chem. Soc., 1958, 80, 4767-4772.

(71) Basu, G.; Cook, G.M.; Belford, R.L. Inorg. Chem., 1964, 3, 1361-1368.

(72) Zahner, J.C.; Drickamer, H.G. J. Chem. Phys., 1960, 33, 1625-1628.

(73) a. Day, P. in reference 3c., p. 191.
b. Beattie, J.K.; Hush, N.S.; Taylor, P.R. Inorg. Chem., 1976, 15, 992-993.
c. Hush, N.S. Prog. Inorg. Chem., 1967, 8, 391-444.
d. Robin, M.B.; Day, P. Advan. Inorg. Chem. Radiochem., 1967, 10, 247-422.
e. The thermal parameters in the $Ni(dpg)_2$ portion of the $Ni(dpg)_2I$ low-temperature structure gave no evidence of metrically nonequivalent sites, which might arise in a trapped valence situation.

(74) Stojakovic, D. R., Ph.D. Thesis, Northwestern University, Evanston, Illinois, August 1977.

(75) Such studies are in progress.

(76) a. Swingle, R. S., II; Riggs, W.M. Critical Rev. Anal. Chem., 1975, 5, 267-321.
b. Jolly, W.L. Topics Curr. Chem., 1977, 71, 149-182.
c. Jolly, W.L. Coord. Chem. Rev., 1974, 13, 47-81.
d. Hercules, D.M.; Carver, J.C. Anal. Chem., 1974, 46, 133R-150R.

(77) a. Cowan, D.O.; Park, J.; Barber, M.; Swift, P. J. Chem. Soc. Chem. Comm., 1971, 1444-1446.
b. Cahen, D.; Lester, J.E. Chem. Phys. Lett., 1973, 18, 108-111.
c. Burroughs, P.; Hammett, A.; Orchard, A.F. J. Chem. Soc. Dalton Trans., 1974, 565-567.
d. Thomas, J.M.; Tricker, M.J. J. Chem. Soc. Faraday Trans. II, 1975, 329-336.
e. Helmer, J.E. J. Electron Spectrosc. Relat. Phenom., 1973, 1, 259-267.
f. Oku, M.; Hirokawa, K. J. Electron. Spectrosc. Relat. Phenom., 1976, 8, 475-481.

(78) Orchard, A.F.; Thornton, G. J. Chem. Soc. Dalton Trans., 1977, 1238-1240.

(79) Hush, N.S. Chem. Phys., 1975, 10, 361-366.

(80) Matienzo, L.J.; Yin, L.I.; Grim, S.O.; Swartz, W.D. Inorg. Chem. 1973, 12, 2762-2769.

(81) a. Kumar, G.; Blackburn, J.R.; Albridge, R.G.; Moddeman, W.E.; Jones, M.M. Inorg. Chem., 1972, 11, 296-300.
b. Clark, D.T.; Adams, D.B. J. Chem. Soc. Chem. Comm., 1971, 602-604.

(82) c. Hedman, Jr.; Klasson, M.; Nilsson, R.; Nordling, C.; Sorokina, M. F.; Kljushnikov, O. I.; Nemnonov, S. A.; Trapeznikov, V. A.; Zyryanov, V. G. Physica Scripta, 1971, 4, 195-201.

(83) a. Lin, L. I.; Ghose, S.; Adler, I. Appl. Spectrosc., 1972, 26, 355-357.
b. Kim, K. S.; Baitinger, W. E.; Amy, J. W.; Winograd, N. J. J. Electron. Spectrosc. Relat. Phenom., 1974, 5, 351-357.

(84) Such behavior is observed for the more conductive, partially oxidized phthalocyanines.[8b]

(85) Drickamer, H. G.; Lynch, R. W.; Clendenen, R. L.; Perez-Albuerne, E. A. Solid State Phys., 1966, 19, 135- .

(86) Kalina, D. W.; Teitelbaum, R. C.; Marks, T. J., unpublished results.

(87) See, for example: Wheland, R. C.; Gillson, J. L. J. Amer. Chem. Soc., 1976, 98, 3916-3925; Chiang, C. K.; Druy, M. A.; Gau, S. C.; Heeger, A. J.; Louis, E. J.; MacDiarmid, A. G.; Park, Y. W.; Shirakawa, H. J. Amer. Chem. Soc., 1978, 100, 1013-1015.

(88) a. Berlinsky, A. J. Contemp. Phys., 1976, 17, 331-354.
b. Thomas, G. A., et al., Phys. Rev. B., 1976, 13, 5105- .
c. Bloch, A. N.; Weisman, R. B.; Varma, C. M. Phys. Rev. Lett., 1972, 28, 753-756.

(89) Shchegolev, I. F. Phys. Stat. Sol. (a), 1972, 12, 9-45.

(90) a. Shante, V. K. S. Phys. Rev. B., 1977, 16, 2597-2612, and references therein.
b. Cohen, M. H. Lecture Notes in Physics, 1977, 65, 225-265, and references therein.
c. Mihaly, G.; Ritvay-Emandity, K.; Janossy, A.; Holczer, K.; Grüner, G. Solid State Comm., 1977, 21, 721-724.
d. Mott, N. F., Metal-Insulator Transitions, Taylor and Francis, London, 1974, Chapt. 1.7.

(91) a. Epstein, A. J.; Conwell, E. M.; Sandman, D. J.; Miller, J. S. Solid State Comm., 1977, 23, 335-358.
b. Epstein, A. J.; Conwell, E. M. Solid State Comm., 1977, 24, 627-630.
c. Conwell, E. M. Phys. Rev. Lett., 1977, 39, 777-780.

(92) Williams, J. M.; Petersen, J. L.; Gerdes, H. M.; Peterson, S. W. Phys. Rev. Lett., 1974, 33, 1079-1081.

(93) Although the observation of a ligand-centered free radical in the EPR spectrum also supports this conclusion, the fact that very pure samples exhibit no signal renders this observation somewhat less meaningful.[14b]

Table I. Summary of Crystal Data, Intensity Data Collection, and Refinement for $Ni(dpg)_2I$ at -160° C

Temperature	-160(5)°C
Formula	$C_{28}H_{22}IN_4NiO_4$
Formula Weight	664.1 amu
Space Group	D_{4h}^8-P4/ncc
a	19.774(8)Å [a]
c	6.446(3)Å
V	2520Å^3
Z	4
Density	1.750g/cm^3 (calc)
Crystal Dimensions	0.53 x 0.04 x 0.04 mm
Crystal Shape	Needle with well developed faces of the forms $\{001\}$, $\{100\}$, and $\{110\}$. [001] is the needle direction
Crystal Volume	0.00051 mm^3
Radiation	Cu Kα_1 (1.540562 Å)
μ	111.8 cm^{-1}
Transmission Factors	0.615-0.731
Receiving Aperture	4.1 x 4.1 mm, 32 cm from crystal
Take-off Angle	3.1°
Scan Speed	1°/min
Scan Range	0.9° below Kα_1 to 0.9° above Kα_2
Background Counts	40s

Table I: Continued.

2θ Limits	2.0° -120.0°
Final Number of Variables	31
Unique Data Used	353
Error in Observation of Unit Weight	4.03 electrons
R	0.093
R_w	0.126

[a]The cell parameters at 23(1)°C are a=19.887(4)Å, c=6.542(2)Å, and V=2587Å^3 .

TABLE II . POSITIONAL AND THERMAL PARAMETERS FOR THE NON-GROUP ATOMS OF BIS(DIPHENYLGLYOXIMATO)NICKEL IODIDE

ATOM	X[A]	Y	Z	B11[B] OR B,A^2	B22	B33	B12	B13	B23
I	1/4	1/4	0.0242(12)	0.99(6)	0.99	102.(3)	0	0	0
NI	-1/4	1/4	-1/4	0.79(10)	0.79	2.4(19)	-0.18(27)	0	0
N	-0.1560(8)	0.2572(10)	-0.2314(28)	0.9(3)					
O	-0.1164(9)	0.2021(9)	-0.238(3)	2.7(4)					
C	-0.1289(10)	0.3180(11)	-0.201(4)	0.3(5)					
H	-0.340	0.340	-1/4	3.7					

[A] ESTIMATED STANDARD DEVIATIONS IN THE LEAST SIGNIFICANT FIGURE(S) ARE GIVEN IN PARENTHESES IN THIS AND ALL SUBSEQUENT TABLES. [B] THE FORM OF THE ANISOTROPIC THERMAL ELLIPSOID IS: $\exp(-(B11H^2+B22K^2+B33L^2+2B12HK+2B13HL+2B23KL))$. THE QUANTITIES GIVEN IN THE TABLE ARE THE THERMAL COEFFICIENTS X 10^3.

TABLE III. DERIVED PARAMETERS FOR THE RIGID GROUP ATOMS OF BIS(DIPHENYLGLYOXIMATO)NICKEL IODIDE

ATOM	X	Y	Z	B, A^2	ATOM	X	Y	Z	B, A^2
C(1)	-0.0584(6)	0.3341(8)	-0.3081(26)	1.2(5)	H(2)	-0.016	0.260	-0.129	2.3
C(2)	-0.0064(7)	0.2949(7)	-0.2262(23)	1.3(5)	H(3)	0.096	0.280	-0.230	2.2
C(3)	0.0602(6)	0.3066(8)	-0.2863(27)	1.2(5)	H(4)	0.120	0.366	-0.469	4.7
C(4)	0.0747(6)	0.3576(9)	-0.4284(28)	3.8(8)	H(5)	0.033	0.432	-0.607	2.4
C(5)	0.0227(8)	0.3968(7)	-0.5103(24)	1.4(5)	H(6)	-0.079	0.412	-0.506	2.0
C(6)	-0.0438(7)	0.3850(7)	-0.4501(25)	1.0(5)					

RIGID GROUP PARAMETERS

GROUP	X_C^A	Y_C	Z_C	$DELTA^B$	EPSILON	ETA
C-RING	0.0082(5)	0.3458(5)	-0.3682(17)	-2.748(11)	-2.499(10)	-2.787(13)
H-RING	0.0082	0.3458	-0.3682	-2.7481	-2.4998	-2.7864

[A] X_C, Y_C, AND Z_C ARE THE FRACTIONAL COORDINATES OF THE ORIGIN OF THE RIGID GROUP. [B] THE RIGID GROUP ORIENTATION ANGLES DELTA, EPSILON, AND ETA (RADIANS) HAVE BEEN DEFINED PREVIOUSLY: S.J. LA PLACA AND J.A. IBERS, ACTA CRYSTALLOGR., 18, 511(1965).

Table IV. Root-Mean-Square Amplitudes of Vibration (Å) of $Ni(dpg)_2I$ at 23°C and -160°C

Atom	Temp. (°C)	Minimum	Intermediate	Maximum
I	23	0.234(4)	0.234	0.756(11)
Ni	23	0.13(2)	0.17(2)	0.21(2)
I	-160	0.140(4)	0.140	0.462(8)
Ni	-160	0.07(3)	0.11(3)	0.14(2)

Table V. Selected Distances and Angles in $Ni(dpg)_2I$ at -160°C

Bond Distances (Å)

Ni-N	1.868(15)	C-C'[a]	1.61(4)
N-O	1.34(2)	C-C(1)	1.59(2)
N-C	1.33(3)	O-H	1.20

Non-Bonded Contacts (Å)

I-I	3.223(2)	C(1)-C(6)'	3.14(2)
Ni-Ni	3.223(2)	C(1)-O	2.89(2)
O-O'''	2.40(4)	C(2)-O	2.85(2)
O-H(2)	2.39	C(6)-O	2.91(2)
C(1)-H(6)'	2.72	C(6)-C	2.91(3)
C(1)-C(1)'	3.10(3)	C(6)-C(1)'	3.14(2)

Angles (deg)

N-Ni-N'	81.5(12)	N-C-C'	105.7(13)
N-Ni-N'''	99.0(12)	N-C-C(1)	118.1(18)
N-Ni-N''	172.7(11)	C'-C-C(1)	105.9(16)
Ni-N-O	121.1(15)	C-C(1)-C(2)	112.0(14)
Ni-N-C	118.6(15)	C-C(1)-C(6)	127.7(13)

Table V: Continued.

Torsion Angles (deg)			
O-N-N''-O''	-176(2)	C(1)-C-C'-C(1)'	-75(2)
O-N-N'''-O'''	2(2)	C(2)-C(1)-C-C'	175(2)
N-C-C'-N'	33(2)	C(2)-C(1)-C-N	-66(2)

[a] Primed atoms are related by the 2-fold axes at $-\frac{1}{4}, \frac{1}{4}, -\frac{1}{4}$. See Figure 3 for the numbering scheme of the $Ni(dpg)_2^+$ cation.

Table VI. Weighted Least-Squares Planes.

Plane equation: $Ax + By + Cz - D = 0$, with x,y,z, in crystal coordinates

Plane No.	A, Å	B, Å	C, Å	D, Å	
1	2.130	-2.130	-6.370	0.528	
2	2.130	-2.130	6.370	-2.657	
3	1.088	1.088	6.426	-1.607	
4	1.088	1.088	-6.426	1.607	
5	0.000	0.000	6.446	-1.612	
6	2.091	12.891	4.840	2.693	Phenyl
7	12.891	2.091	-4.840	-0.287	Phenyl'

Deviations from the Planes (Å) x 10^2

Atom	Plane No. 1	2	3	4	5
Ni					0
N	7(2)			-1(2)	12(2)
O				1(2)	
C	-20(3)				
N'	-7(2)		-1(2)		-12(2)
O'			1(2)		
C'	20(3)				
N''		-7(2)	1(2)		12(2)
O''			-1(2)		
C''		20(3)			
N'''		7(2)		1(2)	-12(2)
O'''				-1(2)	
C'''		-20(3)			

Table VI: Continued.

Dihedral Angles Between Planes

Plane A	Plane B	Angle (deg)	Plane A	Plane B	Angle (deg)
1	2	162.5	3	4	171.1
1	6	143.2	6	7	115.2

Table VII. Raman Scattering Data[a,b]

$Ni(dpg)_2$: 418(ms), 113(w,br), 91(vvw), 71(vw)

$Ni(dpg)_2I$: 447(w), 407(vw), 325(mw,br), 270(w,br), 210(vw,br), 162(vs), 107(w)

$Pd(dpg)_2$: 405(vw), 166(vw), 133(vw), 82(w,sh), 69(vw).

$Pd(dpg)_2I$: 467(vvw), 446(vw), 427(vvw), 323(mw), 266(w,br), 210(vw,br), 160(vs), 104(mw).

(Trimesic acid · $H_2O)_{10}$ · HI_5: 206(w,br), 162(vs), 104(w,br), 75(vw).

[a]Polycrystalline samples, 5145Å excitation.

[b]In cm^{-1}; s = strong, m = medium, w = weak, v = very, br = broad, sh = shoulder

Table VIII. Iodine -129 Mössbauer Parameters.

Compound	$Ni(dpg)_2I$	$Pd(dpg)_2I$	(Trimesic acid · $H_2O)_{10}H^+I_5^-$
Site 1			
δ(mm/sec)[a]	1.20(3)	1.19(3)	1.15(3)
e^2qQ(MHz.)[b]	-1778 (5)	-1749(5)	-1777(5)
B(mm/sec)[c]	1.24(5)	1.36(7)	1.15(5)
Relative population	2.12 (10)	1.96(10)	1.96(10)
Site 2			
δ(mm/sec)	0.47(5)	0.57(5)	0.53(5)
e^2qQ(MHz.)	-1308(8)	-1354(8)	-1404(8)
B(mm/sec)	1.68(5)	1.34(5)	1.75(5)
Relative population	2.22 (10)	1.78(10)	1.97(10)
κ[d]	0.257(5)	0.209(9)	0.138(5)
Site 3			
δ(mm/sec)	0.161(8)	0.201(10)	0.13(5)
e^2qQ(MHz.)	-861(5)	-898(6)	-965(5)
B(mm/sec.)	1.06(4)	1.01(4)	1.04(4)
Relative population	1.00	1.00	1.00
Misfit (%)[d]	0.65(3)	0.64(3)	0.70(4)
χ^2	2856	2112	1400

[a] Versus ZnTe.

[b] For ^{129}I

[c] Linewidth

[d] Defined in Experimental section.

Table IX. Electronic Spectral Data in nm(kK).

Compound	Nujol mull	$CHCl_3$ solution
$Ni(dpg)_2$	285 (35.1)	273 (36.6)
	335 sh (29.9)	357 (28.0)
	372 sh (26.9)	405 (24.7)
	435 (23.0)	460 sh (21.7)
	515 (19.4)	
$Ni(dpg)_2I$	286 (34.9)	
	370 sh (27.0)	
	443 (22.6)	
	520 (19.2)	
	566 (17.7)	
	675 br (15.4)	
$Pd(dpg)_2$	235 (42.6)	243 (41.1)
	278 (36.0)	266 (37.6)
	365 (27.4)	324 (30.9)
	445 (22.5)	410 sh (24.4)
$Pd(dpg)_2I$	235 (42.6)	
	278 (36.0)	
	362 (27.6)	
	456 sh (21.9)	
	505 br (19.8)	
	675 (15.4)	

Table X. X-Ray Photoelectron Spectroscopic Data For Metal Diphenylglyoximates

Material	Ionization	Binding Energy (eV)	FWHM[a](eV)
$Ni(dpg)_2$	Ni $2p_{3/2}$	855.5(5)	1.88
$Ni(dpg)_2I$	Ni $2p_{3/2}$	855.3(5)	1.86
$Pd(dpg)_2$	Pd $3d_{3/2}, 3d_{5/2}$	343.8(4), 338.6(4)	1.88, 1.87
$Pd(dpg)_2I$	Pd $3d_{3/2}$, $3d_{5/2}$	343.(8)(4), 338.8(4)	1.84, 1.85

[a]Full peak width at half maximum.

Table XI. Single Crystal (c axis) Electrical Conductivity Data for Metal Diphenylglyoximates

Material	dc Conductivity at 300°K $(\Omega\text{-cm})^{-1}$ [a]	Conductivity Comparison at 300°K $(\Omega\text{-cm})^{-1}$ [b] dc	ac (100Hz)	Δ(eV)[c]
$Ni(dpg)_2$	$< 8 \times 10^{-9}$			
$Ni(dpg)_2I$	$2.3 - 11 \times 10^{-2}$	2.7×10^{-3}	3.0×10^{-3}	0.19 ± 0.01
$Pd(dpg)_2$	$< 8 \times 10^{-9}$			
$Pd(dpg)_2I$	$7.7 - 47 \times 10^{-4}$	4.7×10^{-4}	5.0×10^{-4}	0.54 ± 0.11

[a] Range given for specimens examined.

[b] Data for the same crystal

[c] From least-sqaures fit to equation 10.

Table XII. Approximate Carrier Mean Free Paths for Some Stacked Conductors at 300°K. [a]

Material	Mean Free Path (Å)
$[(C_2H_5)_2TCC](TCNQ)_2$	2.3×10^{-6} [b]
$Ni(dpg)_2I$	$2.0 \times 10^{-3} - 4.0 \times 10^{-4}$ [c]
$Pd(dpg)_2I$	$8.0 \times 10^{-5} - 1.3 \times 10^{-5}$ [c]
$[(C_2H_5)_3NH](TCNQ)_2$	1.4×10^{-2} [d]
$Qn(TCNQ)_2$	0.43 [e]
(TTF)(TCNQ)	2.3 - 3.5 [f]
NiPcI	3.3 - 8.2 [g]
TTT_2I_3	5.7 - 8.6 [h]
Ni metal	60 [i]

[a] Calculated from equation (II) using data from the sources indicated.

[b] TCC = 3,3-diethylthiacarbocyaninium; Fedutin, D. N.; Shchegolev, I. F.; Stryukov, V. B.; Yagubskii, E. B.; Zvarykina, A. F.; Atovmyam, L. O.; Kaminski, V. F.; Shivaeva, R. P. Phys. Stat. Sol, (b), 1971, 48, 87-92.

[c] This work.

[d] Reference and Kobayashi, H.; Ohashi, Y.; Marumo, F.; Saito, Y. Acta Cryst., 1970, B26, 459-467.

[e] Reference and Kobayashi, H.; Marumo, F.; Saito, Y. Acta Cryst. 1971, B27, 373-378.

[f] Reference 88b.

[g] Reference 8b.

[h] References 4c and 29b.

[i] Reference 38.

Figure 1. A stereo view of the unit cell of $Ni(dpg)_2I$. The a-axis is horizontal to the right, the b-axis is vertical from bottom to top, and the c-axis is towards the reader. The vibrational ellipsoids are drawn at the 50% level, except hydrogen atoms which are drawn arbitrarily small.

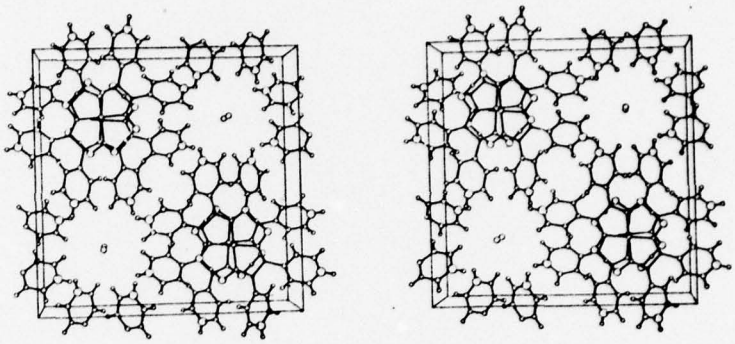

Figure 2. A stereo view of the unit cell of $Ni(dpg)_2I$. The $\underline{a}$-axis is horizontal to the right, the $\underline{b}$-axis is away from the reader, and the $\underline{c}$-axis is vertical from bottom to top. The vibrational ellipsoids of the Ni and I atoms are drawn at the 50% level. All other atoms are drawn arbitrarily small.

Top

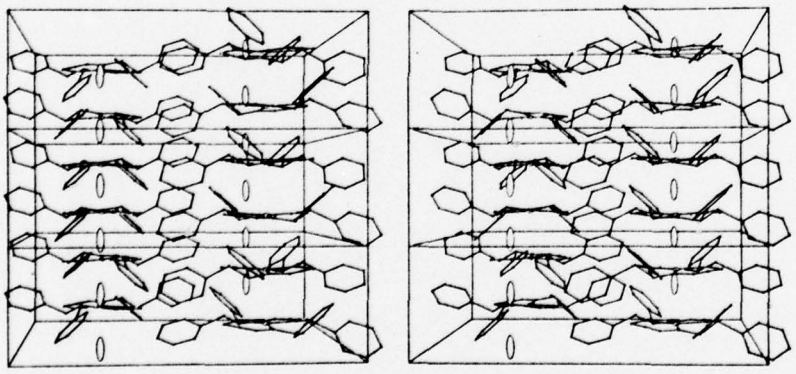

Figure 3. A drawing of the $Ni(dpg)_2^{+0.20}$ cation showing the numbering scheme used and some relevant bond lengths and angles. The vibrational ellipsoids are drawn at the 50% level, except hydrogen atoms which are arbitrarily small.

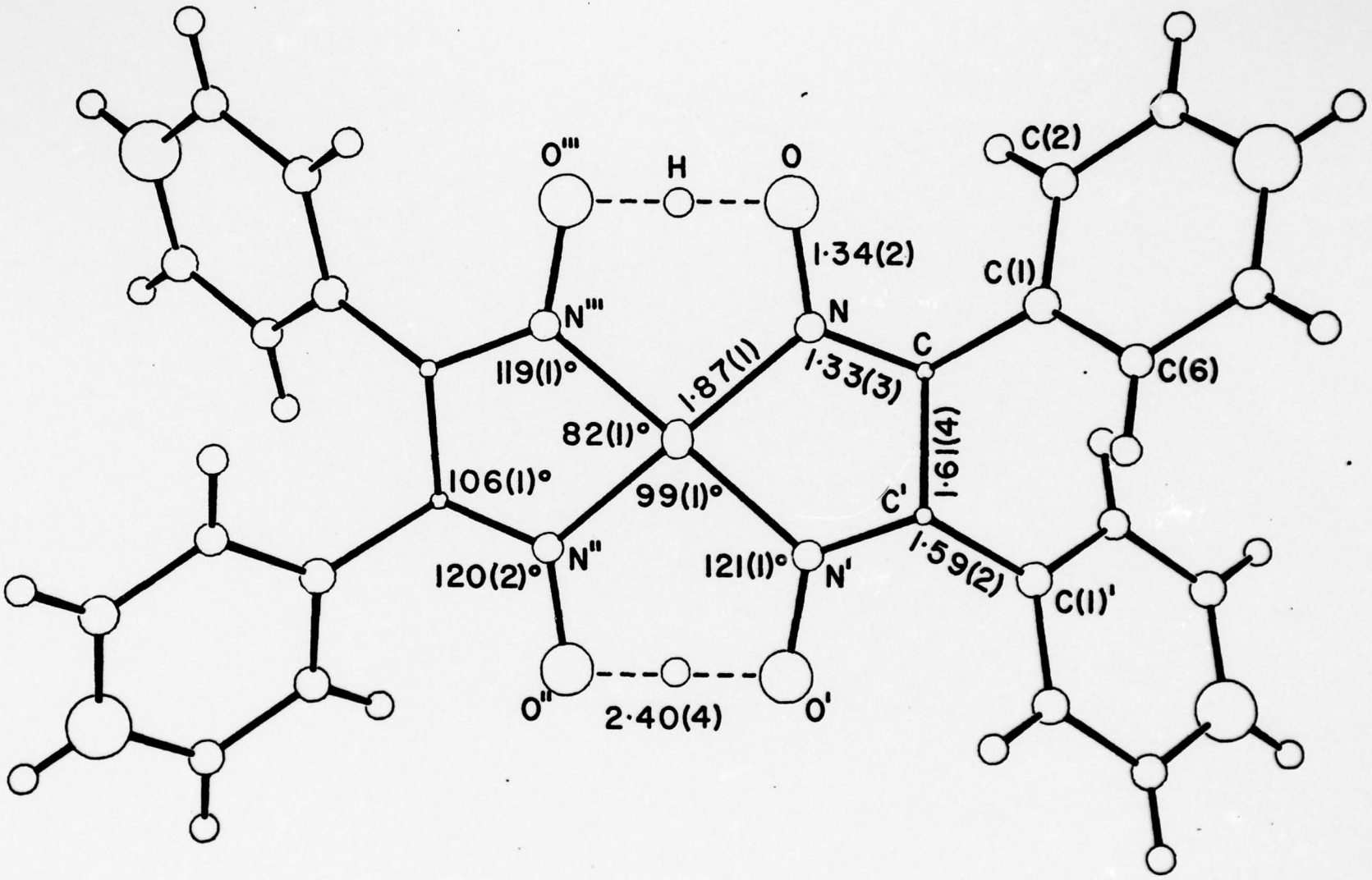
O'''
H
O
C(2)
1·34(2)
C(1)
N'''
N
C
C(6)
119(1)°
1·87(1)
1·33(3)
82(1)°
1·61(4)
106(1)°
99(1)°
C'
N''
120(2)°
121(1)°
N'
1·59(2)
C(1)'
O''
2·40(4)
O'

Figure 4. Resonance Raman spectra (5145Å excitation) of A. I_2 dissolved in benzene, B. Polycrystalline $(C_6H_5)_4As^+I_3^-$, C. Polycrystalline $(C_6H_5CONH_2)_2H^+I_3^-$, D. Polycrystalline $Cs^+I_3^-$, E. Polycrystalline $(phenacetin)_2H^+I_3^- \cdot I_2$, F. Polycrystalline $(trimesic\ acid \cdot H_2O)_{10}H^+I_5^-$.

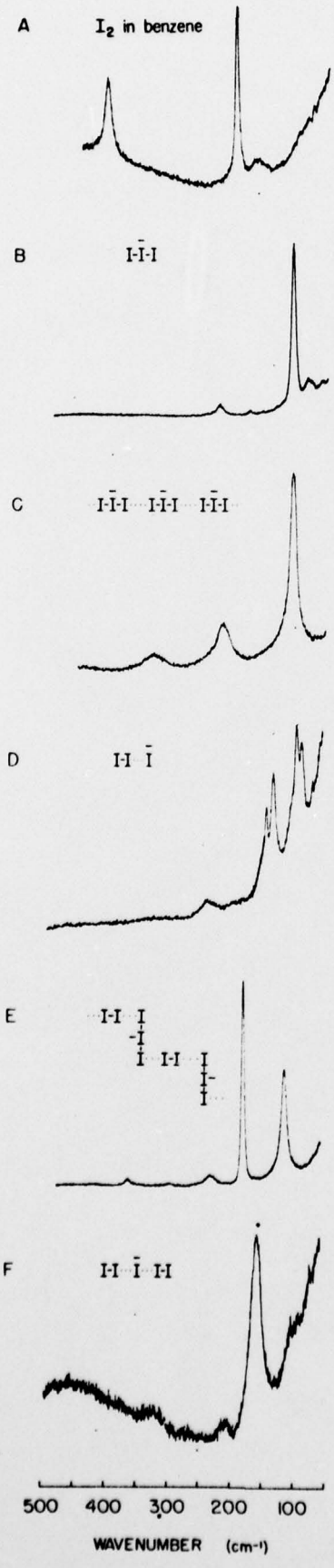
A
I_2 in benzene
B
I-I-I
C
I-I-I I-I-I I-I-I
D
I-I I
E
I-I
I I-I
F
I-I I I-I
500 400 300 200 100
WAVENUMBER (cm-1)

Figure 5. Raman spectra (5145Å excitation, polycrystalline samples) of

A. $Pd(dpg)_2I$, B. $Pd(dpg)_2$,

C. $Ni(dpg)_2I$, D. $Ni(dpg)_2$.

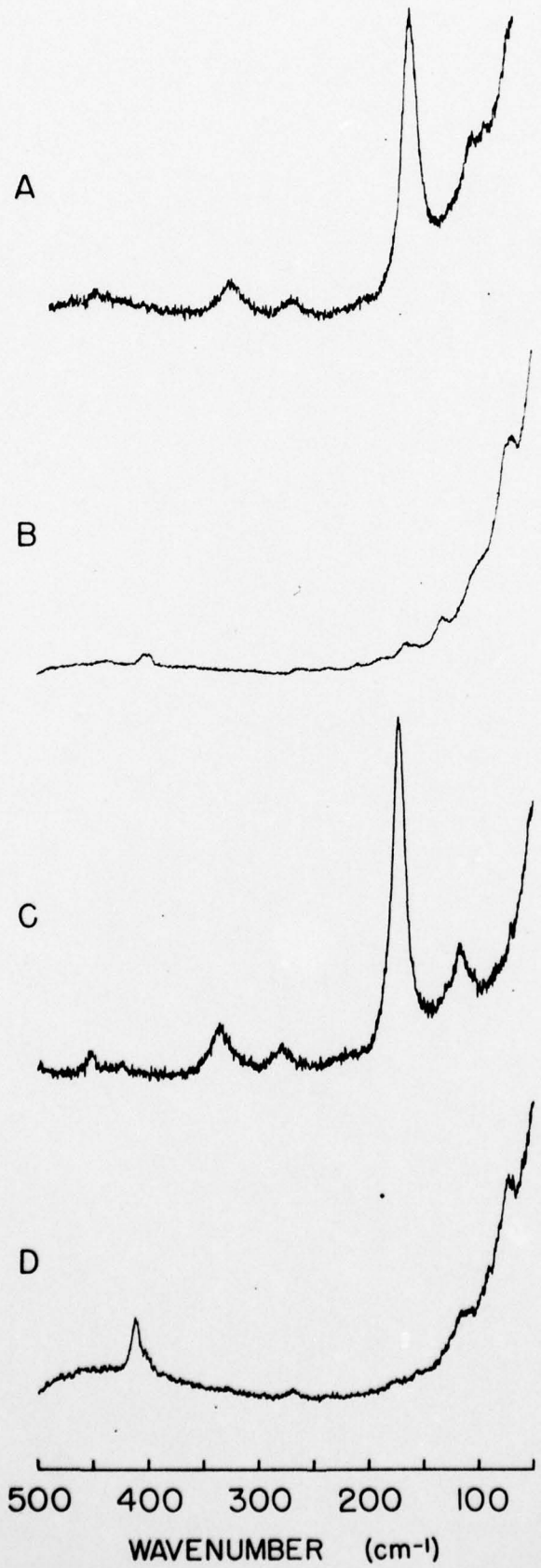
A
B
C
D
500
400
300
200
100
WAVENUMBER (cm-1)

Figure 6. Iodine -129 Mössbauer spectra of the indicated compounds as solids at 4°K. The solid lines represent the best computer fit to the data points. Stick figures representing contributing transitions are shown for the $Ni(dpg)_2I$ spectrum. Isomer shifts are referenced to ZnTe.

^{129}I MÖSSBAUER SPECTRA

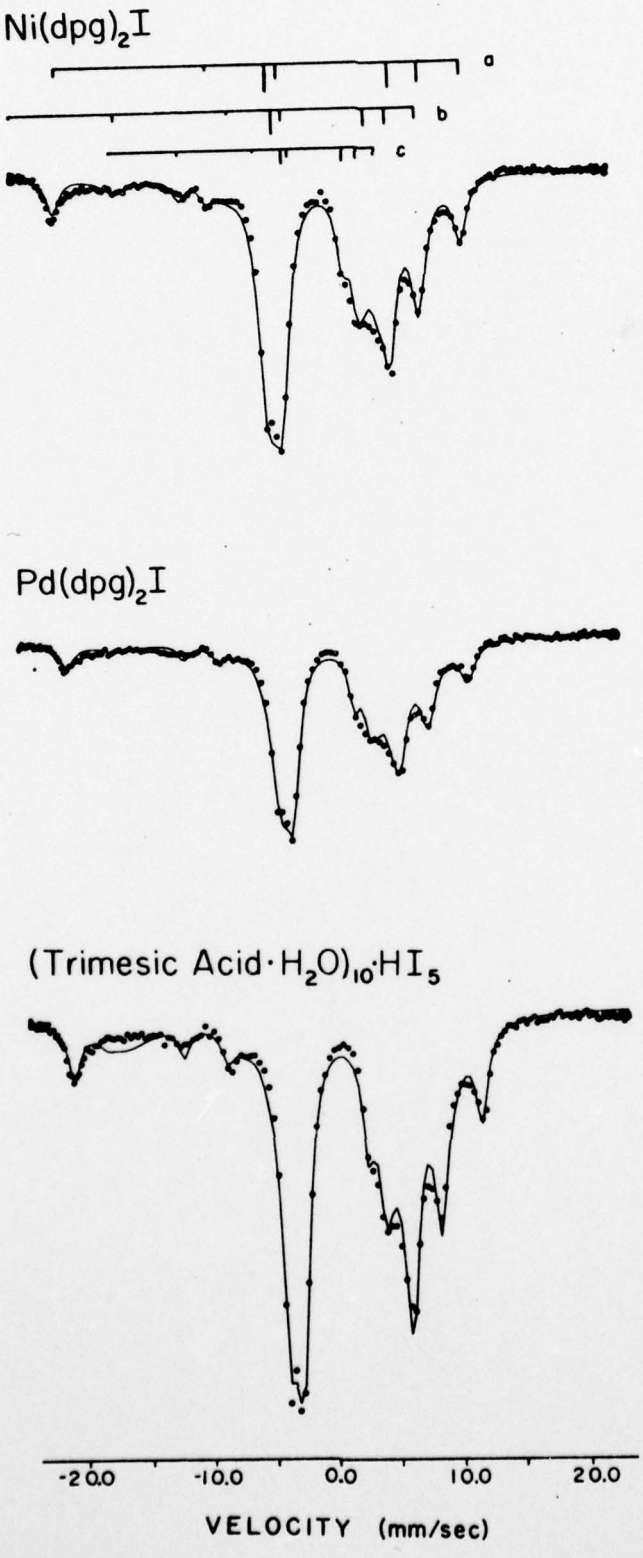

Figure 7. Electronic spectra (polycrystalline samples as Nujol mulls) of A. $Pd(dpg_2)I$ B. $Pd(dpg)_2$ C. $Ni(dpg)_2I$ D. $Ni(dpg)_2$ E. $(Trimesic\ acid \cdot H_2O)_{10}H^+I_5^-$.

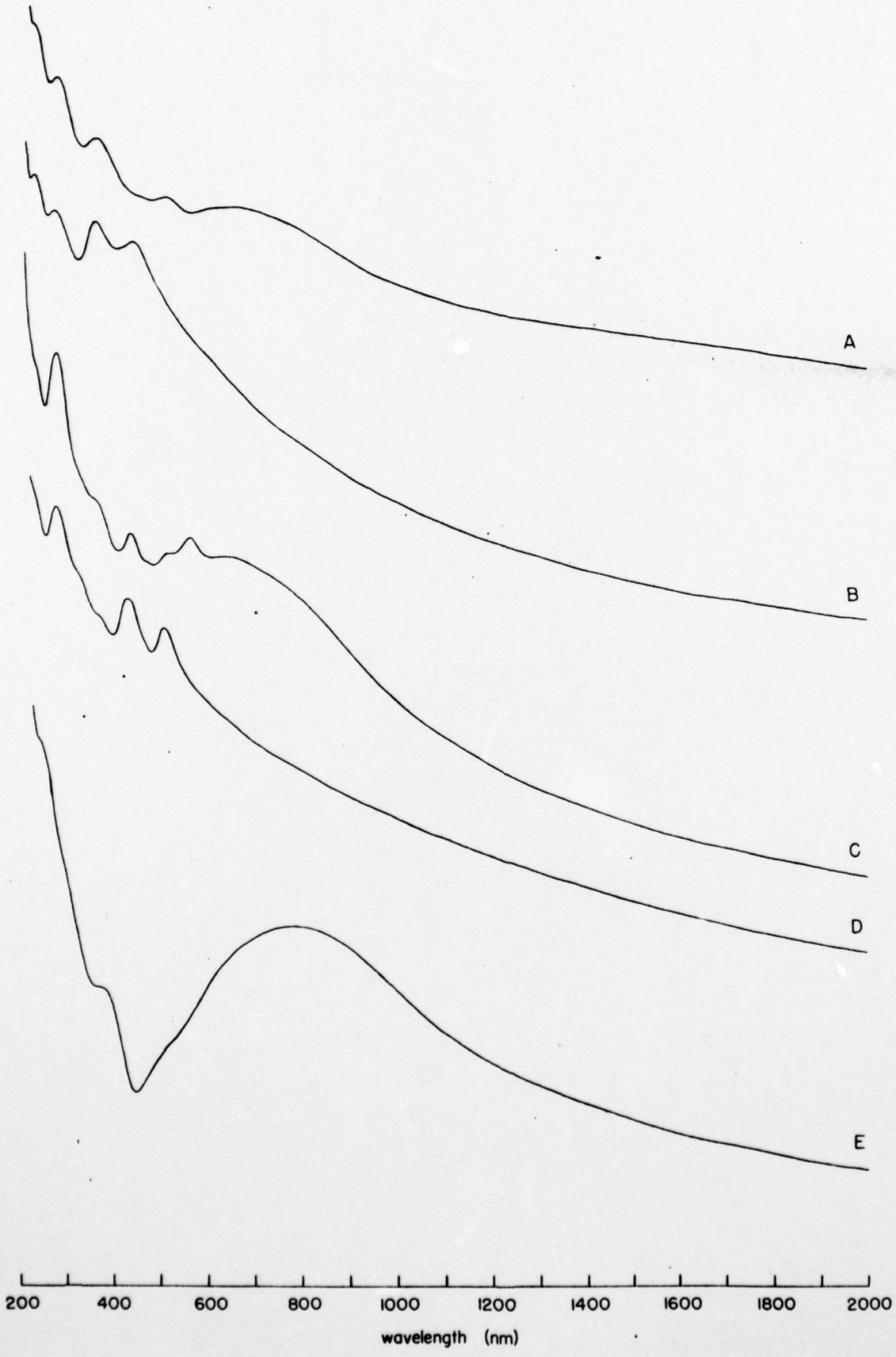
A
B
C
D
E
200
400
600
800
1000
1200
1400
1600
1800
2000
wavelength (nm)

Figure 8. X-ray photoelectron spectra of the indicated compounds in $2p_{3/2}$ (Ni) and $3d_{5/2}$, $3d_{3/2}$ (Pd) regions. Traces are the result of 100-200 computer-averaged scans.

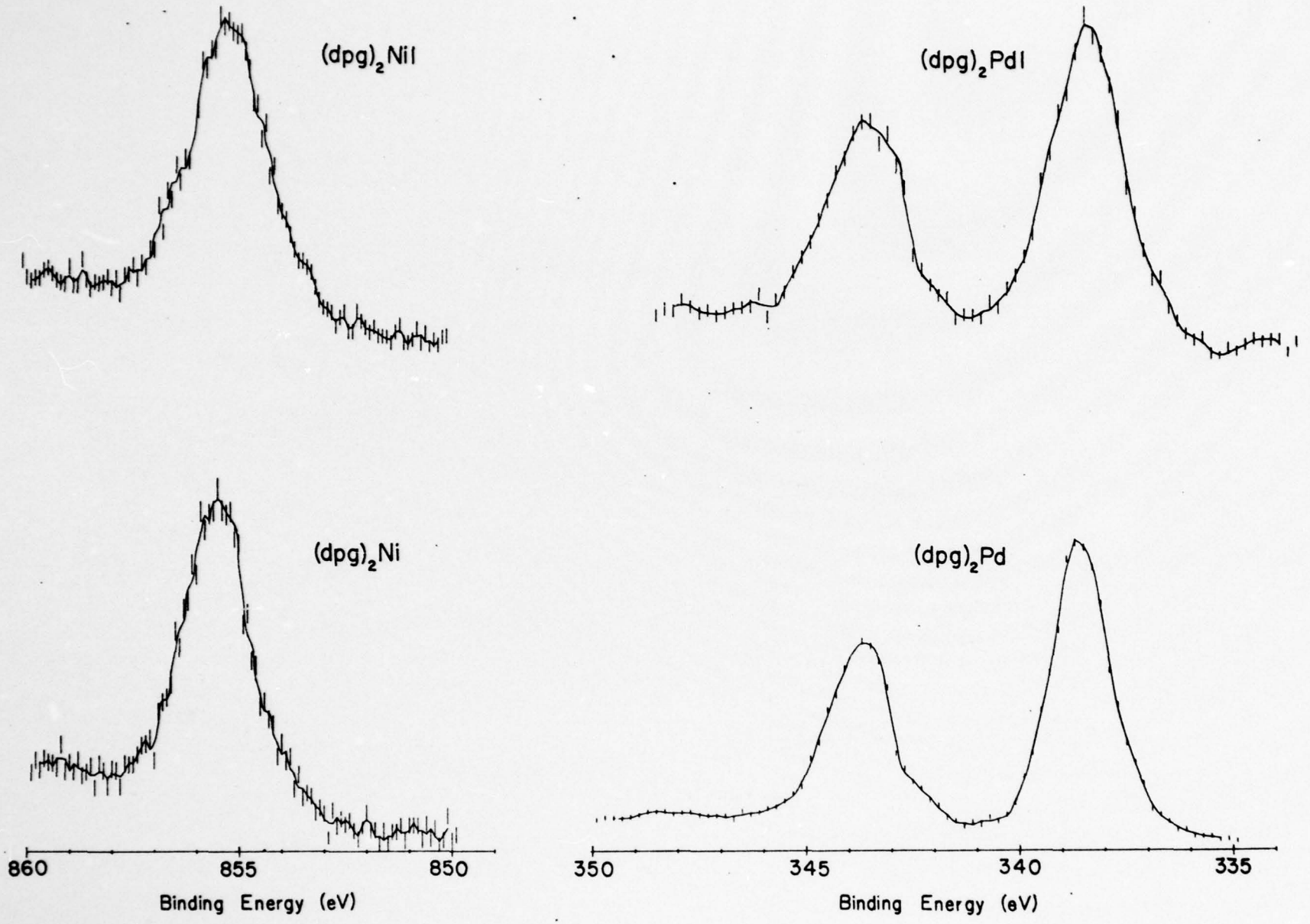
(dpg)2NiI
(dpg)2PdI
(dpg)2Ni
(dpg)2Pd
860
855
850
Binding Energy (eV)
350
345
340
335
Binding Energy (eV)

Figure 9. Electrical conductivity (dc) in the crystallographic c direction of representative $Ni(dpg)_2I$ crystals as a function of temperature.

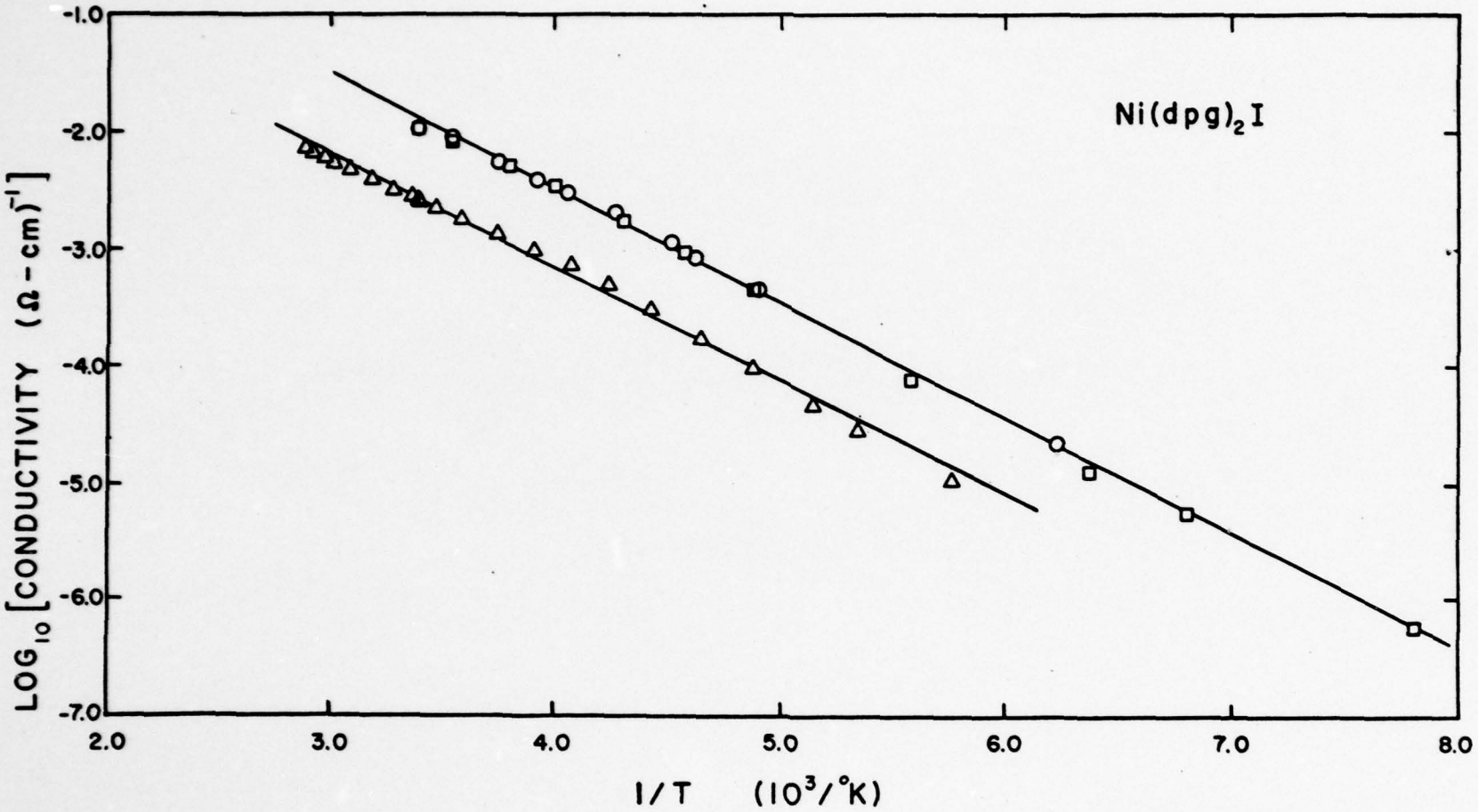
Ni(dpg)2I
LOG10 [CONDUCTIVITY (Ω-cm)-1]
-1.0
-2.0
-3.0
-4.0
-5.0
-6.0
-7.0
2.0
3.0
4.0
5.0
6.0
7.0
8.0
1/T (10³/°K)

Figure 10. Electrical conductivity (dc) in the crystallographic c direction of representative $Pd(dpg)_2I$ crystals as a function of temperature.

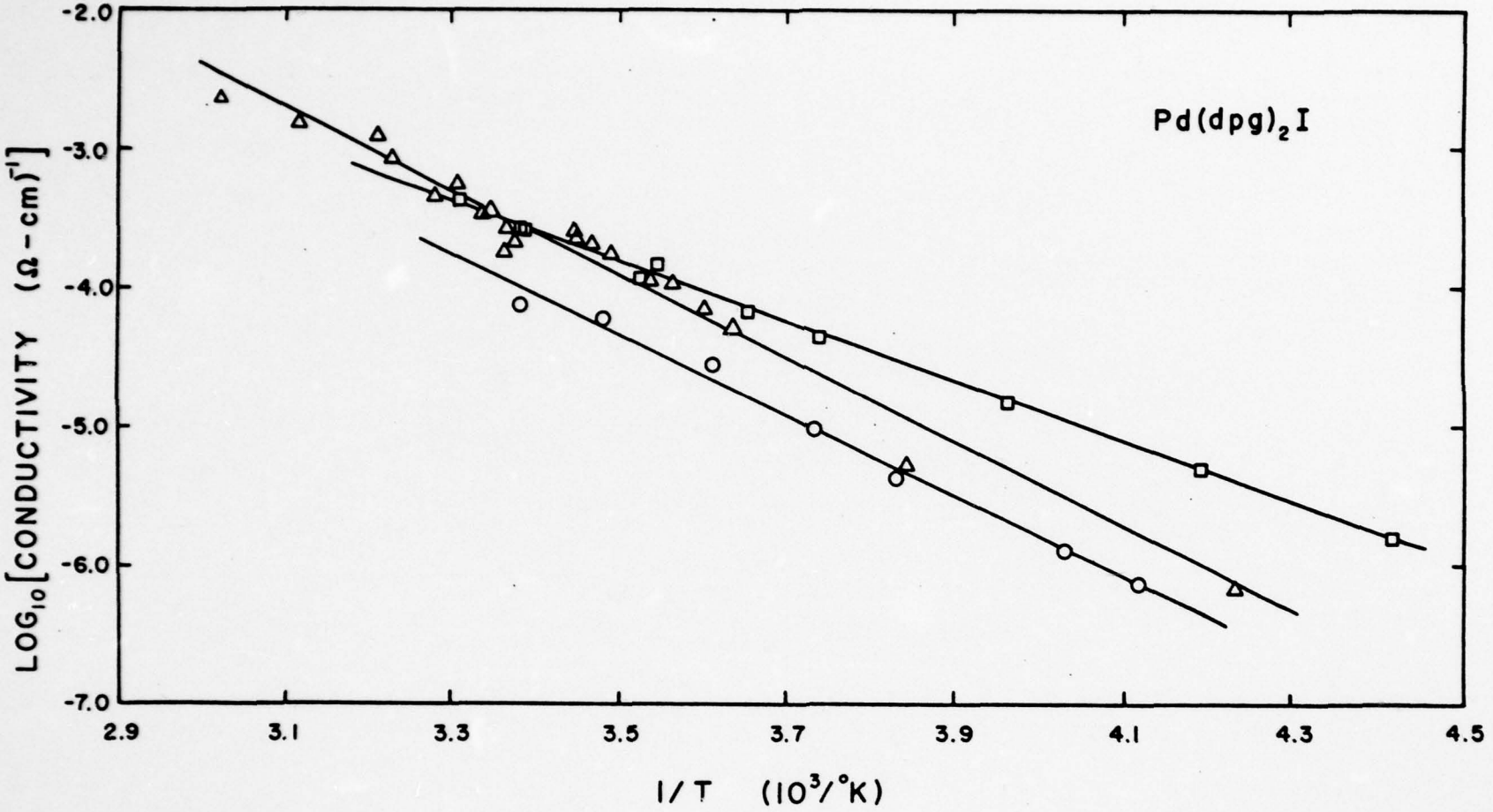
Pd(dpg)2I
LOG10[CONDUCTIVITY (Ω-cm)-1]
-2.0
-3.0
-4.0
-5.0
-6.0
-7.0
2.9
3.1
3.3
3.5
3.7
3.9
4.1
4.3
4.5
1/T (10³/°K)

AD-A059 641 NORTHWESTERN UNIV EVANSTON ILL DEPT OF CHEMISTRY F/G 7/2
RATIONAL SYNTHESIS OF UNIDIMENSIONAL MIXED VALENCE SOLIDS. STRU--ETC(U)
AUG 78 M A COWIE, A GLEIZES, G W GRYNKEWICH N00014-77-C-0231
UNCLASSIFIED TR-5 NL

2 OF 2
AD
A059641

END
DATE
FILMED
12-78
DDC

TECHNICAL REPORT DISTRIBUTION LIST

	No. Copies
Office of Naval Research Arlington, Virginia 22217 Attn: Code 472	2
Office of Naval Research Arlington, Virginia 22217 Attn: Code 102IP 1	6
ONR Branch Office 536 S. Clark Street Chicago, Illinois 60605 Attn: Dr. Jerry Smith	1
ONR Branch Office 715 Broadway New York, New York 10003 Attn: Scientific Dept.	1
ONR Branch Office 1030 East Green Street Pasadena, California 91106 Attn: Dr. R. J. Marcus	1
ONR Branch Office 760 Market Street, Rm. 447 San Francisco, California 94102 Attn: Dr. P. A. Miller	1
ONR Branch Office 495 Summer Street Boston, Massachusetts 02210 Attn: Dr. L. H. Peebles	1
Director, Naval Research Laboratory Washington, D.C. 20390 Attn: Code 6100	1
The Asst. Secretary of the Navy (R&D) Department of the Navy Room 4E736, Pentagon Washington, D.C. 20350	1
Commander, Naval Air Systems Command Department of the Navy Washington, D.C. 20360 Attn: Code 310C (H. Rosenwasser)	1
Defense Documentation Center Building 5, Cameron Station Alexandria, Virginia 22314	12
U.S. Army Research Office P.O. Box 12211 Research Triangle Park, N.C. 27709 Attn: CRD-AA-IP	1
Naval Ocean Systems Center San Diego, California 92152 Attn: Mr. Joe McCartney	1
Naval Weapons Center China Lake, California 93555 Attn: Head, Chemistry Division	1
Naval Civil Engineering Laboratory Port Hueneme, California 93041 Attn: Mr. W. S. Haynes	1
Professor O. Heinz Department of Physics & Chemistry Naval Postgraduate School Monterey, California 93940	1
Dr. A. L. Slafkosky Scientific Advisor Commandant of the Marine Corps (Code RD-1) Washington, D.C. 20380	1
Office of Naval Research Arlington, Virginia 22217 Attn: Dr. Richard S. Miller	1

TECHNICAL REPORT DISTRIBUTION LIST

	No. Copies
Dr. R. M. Grimes University of Virginia Department of Chemistry Charlottesville, Virginia 22901	1
Dr. M. Tsutsui Texas A&M University Department of Chemistry College Station, Texas 77843	1
Dr. C. Quicksall Georgetown University Department of Chemistry 37th & O Streets Washington, D.C. 20007	1
Dr. M. F. Hawthorne University of California Department of Chemistry Los Angeles, California 90024	1
Dr. D. B. Brown University of Vermont Department of Chemistry Burlington, Vermont 05401	1
Dr. W. B. Fox Naval Research Laboratory Chemistry Division Code 6130 Washington, D.C. 20375	1
Dr. J. Adcock University of Tennessee Department of Chemistry Knoxville, Tennessee 37916	1
Dr. A. Cowley University of Texas Department of Chemistry Austin, Texas 78712	1
Dr. W. Hatfield University of North Carolina Department of Chemistry Chapel Hill, North Carolina 27514	1
Dr. D. Seyferth Massachusetts Institute of Technology Department of Chemistry Cambridge, Massachusetts 02139	1
Dr. M. H. Chisholm Princeton University Department of Chemistry Princeton, New Jersey 08540	1
Dr. B. Foxman Brandeis University Department of Chemistry Waltham, Massachusetts 02154	1
Dr. T. Marks Northwestern University Department of Chemistry Evanston, Illinois 60201	1
Dr. G. Geoffrey Pennsylvania State University Department of Chemistry University Park, Pennsylvania 16802	1
Dr. J. Zuckerman University of Oklahoma Department of Chemistry Norman, Oklahoma 73019	1